JACS
JOURNAL OF THE AMERICAN CHEMICAL SOCIETY
Article
pubs.acs.org/JACS

Metal-Catalyzed C−C Bond Cleavage in Alkanes: Effects of Methyl Substitution on Transition-State Structures and Stability

David W. Flaherty,[†,‡] David D. Hibbitts,[†] and Enrique Iglesia*[,†]

[†]Department of Chemical Engineering, University of California at Berkeley, Berkeley, California 94720, United States
[‡]Department of Chemical and Biomolecular Engineering, University of Illinois at Urbana−Champaign, Urbana, Illinois 61801, United States

Supporting Information

ABSTRACT: Methyl substituents at C−C bonds influence hydrogenolysis rates and selectivities of acyclic and cyclic C_2−C_8 alkanes on Ir, Rh, Ru, and Pt catalysts. C−C cleavage transition states form via equilibrated dehydrogenation steps that replace several C−H bonds with C-metal bonds, desorb H atoms (H*) from saturated surfaces, and form λ H_2(g) molecules. Activation enthalpies ($\Delta H^{\ddagger}$) and entropies ($\Delta S^{\ddagger}$) and λ values for ^{3}C−^{x}C cleavage are larger than for ^{2}C−^{2}C or ^{2}C−^{1}C bonds, irrespective of the composition of metal clusters or the cyclic/acyclic structure of the reactants. ^{3}C−^{x}C bonds cleave through α,β,γ- or $\alpha,\beta,\gamma,\delta$-bound transition states, as indicated by the agreement between measured activation entropies and those estimated for such structures using statistical mechanics. In contrast, less substituted C−C bonds involve α,β-bound species with each C atom bound to several surface atoms. These α,β configurations weaken C−C bonds through back-donation to antibonding orbitals, but such configurations cannot form with ^{3}C atoms, which have one C−H bond and thus can form only one C−M bond. ^{3}C−^{x}C cleavage involves attachment of other C atoms, which requires endothermic C−H activation and H* desorption steps that lead to larger $\Delta H^{\ddagger}$ values but also larger $\Delta S^{\ddagger}$ values (by forming more H_2(g)) than for ^{2}C−^{2}C and ^{2}C−^{1}C bonds, irrespective of alkane size (C_2−C_8) or cyclic/acyclic structure. These data and their mechanistic interpretation indicate that low temperatures and high H_2 pressures favor cleavage of less substituted C−C bonds and form more highly branched products from cyclic and acyclic alkanes. Such interpretations and catalytic consequences of substitution seem also relevant to C−X cleavage (X = S, N, O) in desulfurization, denitrogenation, and deoxygenation reactions.

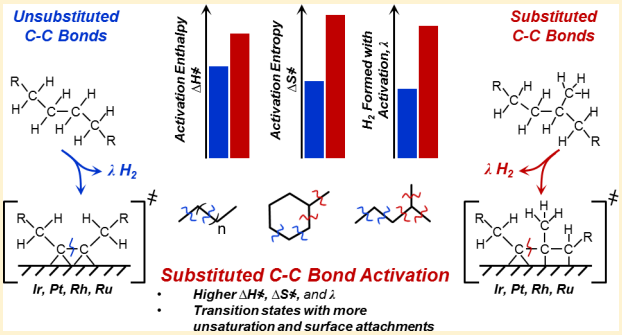

1. INTRODUCTION

Supported metal clusters cleave C−C bonds via hydrogenolysis reactions during catalytic reforming and isomerization processes,[1] which increase fuel octane values by converting *n*-alkanes into arenes, cycloalkanes, and branched acyclic alkanes.[2,3] The rate and location of C−C bond cleavage events in alkanes reflect, in part, the degree of substitution at each C atom in the C−C bond. Specifically, hydrogenolysis rates are lower at more substituted C atoms; for example, the rate of cleavage at terminal methyl groups decreases as vicinal C atoms become more substituted (rates decrease as ^{1}C ≈ ^{2}C > ^{3}C > ^{4}C, where superscripts denote the number of C−C bonds to the C atom).[4] These trends reflect activation enthalpies ($\Delta H^{\ddagger}$) and entropies ($\Delta S^{\ddagger}$) that predominantly depend on the substitution at the two C atoms in the cleaved C−C bond, but $\Delta H^{\ddagger}$ and $\Delta S^{\ddagger}$ values appear to be insensitive to the degree of substitution of C atoms in the alkane that are not part of the cleaved C−C bond.[5] The effects of alkane substitution are also evident in ring-opening reactions of substituted cycloalkanes (e.g., methylcyclohexane, dimethylcyclohexane, bicyclodecane), for which ^{2}C−^{2}C cleavage rates are larger than for ^{3}C−^{2}C bonds and ^{2}C−^{2}C bonds at α-positions to the ^{3}C atom cleave more slowly than those at ^{2}C−^{2}C bonds at the β-position.[6−8] Such results are inconsistent with expectations from linear free energy relations,[9] because homolytic C−C bond dissociation energies (BDE(C−C)) are actually lower for more substituted C atoms,[10] suggesting that intrinsic activation enthalpies (H_{act}) to cleave the C−C bond would also be smaller. $\Delta H^{\ddagger}$ values for C−C bond cleavage increase with increasing average BDE(C−C) values for each *n*-alkane (C_2−C_{10}) on Ir surfaces saturated with chemisorbed hydrogen atoms (H*).[11] Previously observed effects of substitution on $\Delta H^{\ddagger}$ and $\Delta S^{\ddagger}$ values[5] show that BDE(C−C) values[11] are inappropriate descriptors for C−C bond reactivity. Other factors, such as differences in transition-state structures, Pauli exclusion−steric repulsion (from orbital overlaps between alkyl groups attached to the C−C bond and surface metal atoms),[12,13] or differences among BDE(C−M) for C−M bonds that bind the transition state to the metal surface, may instead account for the effects of substitution on C−C bond cleavage rates.

Received: April 14, 2014
Published: June 25, 2014

dx.doi.org/10.1021/ja5037429 | J. Am. Chem. Soc. 2014, 136, 9664−9676

Table 1. Synthesis Conditions and Characterization Results for Metal Cluster Catalysts

			temperature (K)		fractional dispersion				
sample	TEA:M[a]	metal content (% wt)	oxidative treatment[b]	reductive treatment[c]	H_2[d]	O_2[e]	CO[f]	$\langle d_{chem}\rangle$ (nm)[g]	$\langle d_{TEM}\rangle$ (nm)[h]
0.7 nm Ir	20	1.0	573, 1 h	873, 3 h	1.4	1.7	1.5	0.7	0.8
7 nm Ir	10	3.0	1123, 12 h	1173 8 h	0.13	0.15	0.13	7.1	14
0.9 nm Rh	10	0.5	573, 1 h	723, 3 h	1.1	1.2	0.99	0.9	0.9
1.0 nm Ru	10	0.5	573, 1 h	723, 3 h	0.98	1.1	–	1.0	0.9
0.6 nm Pt	–[i]	1.0	–	723, 3 h	1.6	1.6	1.5	0.6	0.7

[a]Ratio of triethanol amine to metal precursor in aqueous solution used for SiO_2 impregnation. [b]21 kPa O_2 (dry air). [c]50 kPa H_2 (balance He). [d]H_2 chemisorption (irreversible uptake at 300 K), assuming $H/M_s = 1$. [e]O_2 chemisorption (irreversible uptake at 300 K), assuming $O/M_s = 1$. [f]CO chemisorption (irreversible uptake at 300 K), assuming $CO/M_s = 1$. [g]Mean particle diameters, $\langle d_{chem}\rangle$, calculated using the irreversible H_2 uptake and assuming hemispherical clusters with densities equal to the bulk metal. [h]Surface-averaged mean particle diameter from TEM analysis, see description of methods (section 2.2). [i]Pt-SiO_2 was prepared using strong-electrostatic adsorption and did not involve TEA.

Previous studies have detected metallacyclic intermediates on metal surfaces using vibrational spectroscopy,[14,15] but analogous transition states have been infrequently implicated for $^3C-^xC$ bond cleavage.[16] Instead, recent computational studies of ring-opening reactions of methylcyclopentane on extended Pt, Rh, Ir, and Pd surfaces[17,18] have suggested that C−C bonds cleave via α,β-coordinated transition states, as determined for $^2C-^2C$, $^2C-^1C$, and $^1C-^1C$ bonds,[19] in contradiction with previous proposals for metallacyclic intermediates with α,γ-coordination.[4,20,21] These theoretical treatments have also proposed that transition states that cleave $^3C-^xC$ bonds form covalent linkages between both C atoms in the cleaved C−C bond and exposed metal atoms,[17,18] as also shown for C−C bond cleavage in *n*-alkanes.[4,11,22] Thus, it seems unlikely that the low reactivity of $^3C-^xC$ bonds relative to less substituted bonds reflects C−C cleavage via metallacyclic transition states.[4]

Differences between the adsorption enthalpies of intermediates that cleave $^3C-^xC$ and less substituted C−C bonds are also unlikely to account for the low reactivity of $^3C-^xC$ bonds compared to $^2C-^2C$ and $^2C-^1C$ bonds. Density functional theory (DFT) derived energies for the bonds between ^3C atoms or ^2C atoms and metal surfaces (i.e., BDE(^{3}C−M) and BDE(^{2}C−M), where M is a surface metal atom)[12,13,23] differ by amounts nearly equal to their respective BDE(^{3}C−H) and BDE(^{2}C−H) values.[10] Consequently, the overall enthalpy change associated with dehydrogenation of a given isoalkane and the adsorption of the dehydrogenated intermediate onto a metal surface is unaffected by the substitution at the C atoms bound to the surface. Studies of organometallic complexes[24,25] and recent microcalorimetric results[26] show that differences among bond energies for organic fragments (e.g., BDE(C−M), BDE(RO−M)) at metal centers or metal surfaces are equal to the differences between bonds to hydrogen atoms (e.g., BDE(C−H), BDE(RO−H)) at the same intramolecular positions. These results indicate that bond enthalpy differences cannot account for the very different stabilities of the transition states that mediate $^3C-^xC$ and $^2C-^2C$ or $^2C-^1C$ bond cleavage (i.e., a strong C−H bond is replaced with a strong C−M bond, such that reaction enthalpies are equal at ^1C, ^2C, or ^3C atoms).[5,20] Therefore, we conclude that the marked differences in hydrogenolysis turnover rates among these types of C−C bonds cannot reflect differences between BDE(C−M) and BDE(C−H) values at these C−C bonds.

Here, we seek to resolve these matters by using statistical mechanics formalisms and transition-state theory to interpret these reactivity trends. This approach was recently used to describe enthalpic and entropic barriers for cleaving specific C−C bonds in *n*-alkanes (C_2-C_{10}) on surfaces saturated with chemisorbed hydrogen (H*).[11] In the specific case of ethane, such treatments were combined with DFT calculations to confirm these mechanistic details and to show how the extent of dehydrogenation influences H_{act} values for C−C bond rupture.[19] We report rates for the cleavage of each C−C bond in a series of nine branched, linear, and cyclic alkanes on H*-saturated Ir, Rh, Ru, and Pt clusters and their kinetic dependence on reactant concentrations and temperature. These data show that $^3C-^xC$ cleavage occurs in transition states formed by alkane reactants losing 4−5 H atoms, with each H atom replaced by one C−M bond. $^3C-^xC$ bond cleavage transition states can only form one bond between the ^3C atom and the surface, because only one H atom is available. Therefore, three or more C atoms must lose H atoms and bind to surfaces to account for all the H atoms removed to form these transition states. The binding of these C atoms to H*-covered catalyst surfaces forms C−M bonds at the expense of C−H and M−H bonds; such reactions are endothermic and decrease the entropy of transition states, thus making them less stable. The process of cleaving C−H bonds and binding an unsaturated C atom to a vacancy on H*-covered surfaces, however, increases entropy (by ∼100 J mol^{-1} K^{-1}) because these steps evolve H_2(g) produced by breaking the C−H and M−H bonds. Such entropy gains help to overcome the large $\Delta H^{\ddagger}$ values prevalent for $^3C-^xC$ bond cleavage. $\Delta H^{\ddagger}$ values for $^3C-^xC$ bonds are much larger than for $^2C-^2C$ and $^2C-^1C$ bonds, however, at typical hydrogenolysis temperatures (>500 K) their larger $\Delta S^{\ddagger}$ make activation free energies ($\Delta G^{\ddagger}$) for $^3C-^xC$ bond cleavage comparable to those for less substituted C−C bonds. Together these data and their interpretation show that the inability to form more than a single C−M bond to ^3C atoms gives rise to differences in $\Delta H^{\ddagger}$ and $\Delta S^{\ddagger}$ that can be used to control product formation rates and selectivities during hydrotreating reactions that upgrade fossil and biomass reactants.

2. EXPERIMENTAL PROCEDURES

2.1. Synthesis of Metal Cluster Catalysts. Silica (Davisil 646, 300 m^2 g^{-1}) used to prepare all materials was treated in flowing dry air (Praxair, 99.99%, 5.0 cm^3 g^{-1} s^{-1}) by heating to 823 K at 0.03 K s^{-1} and holding for 5 h. Ir precursors were deposited onto SiO_2 using an aqueous solution prepared by mixing triethanolamine (TEA, Sigma-Aldrich 97%) and H_2IrCl_6 (Strem Chemicals, 99%) (20:1 mol) with deionized water (17.9 MΩ resistivity) using reported methods.[11] This solution was added dropwise onto treated SiO_2 to incipient wetness to prepare Ir-SiO_2 (1.0% wt.). Rh-SiO_2 (0.5% wt.) and Ru-SiO_2 (1.0% wt.) were prepared by impregnating treated SiO_2 with solutions containing TEA and $Rh(NO_3)_3$ (Sigma-Aldrich, 99%) or $Ru(NO)(NO_3)_3$[27] (Sigma-Aldrich, 99%, in dilute HNO_3) in 10:1 mol in DI water. Pt-SiO_2 (1.0% wt.) was synthesized by strong-electrostatic adsorption of Pt-$(NH_3)_4(NO_3)_2$ (Sigma-Aldrich, 99.9%) onto SiO_2 in a 0.4 M

dx.doi.org/10.1021/ja5037429 | J. Am. Chem. Soc. 2014, 136, 9664−9676

NH_4OH solution, as described previously.[11,28] All supported metal samples were heated to 393 K at 0.017 K s^{-1} in flowing dry air (Praxair, 99.99%, 5.0 cm^3 g^{-1} s^{-1}) and held for 8 h. The resulting dry Ir-SiO_2, Rh-SiO_2, and Ru-SiO_2 powders were heated to 573 K at 0.017 K s^{-1} in flowing dry air and held for 1 h to condense TEA complexes with silanols.[27] These samples were then heated to 673 K at 0.033 K s^{-1} in flowing 50% H_2/He (Praxair, 99.999%, 1.0 cm^3 g^{-1} s^{-1}) and held for 3 h to decompose the precursors and form Ir, Rh, and Ru metal clusters. The dried Pt-SiO_2 was heated to 723 K at 0.017 K s^{-1} in flowing 50% H_2/He and held for 3 h to form Pt clusters. All samples were cooled to ambient temperature and passivated in flowing 0.5% O_2/He (Praxair, 99.99%, 1.0 cm^3 g^{-1} s^{-1}) for 6 h before exposure to ambient air. The dispersions of the Ir-SiO_2 were varied by subsequent oxidative and reductive treatments (Table 1).

2.2. Characterization of Metal Cluster Catalysts. The number of exposed metal surface atoms (M_s) for each catalyst was determined from measured volumetric uptakes of H_2, O_2, and CO at 298 K.[11,29] Mean metal cluster diameters ($\langle d_{chem} \rangle$) were estimated from chemisorption uptakes by assuming hemispherical crystallites. The $\langle d_{chem} \rangle$ values of Ir, Ru, Rh, and Pt clusters determined from H_2, O_2, and CO chemisorption are shown in Table 1. The mean values of $\langle d_{chem} \rangle$, calculated from the results of all three titrants, are 0.7 and 7 nm for the two Ir samples, and 0.9, 1.0, and 0.7 nm for the Rh, Ru, and Pt samples, respectively.

Cluster size distributions were measured from TEM images in bright-field mode (Philips, CM200F) using samples dispersed as fine dust onto a Cu grid coated with lacey carbon. The surface-averaged cluster diameter ($\langle d_{TEM} \rangle$) was calculated using

$$\langle d_{TEM} \rangle = \frac{\sum n_i d_i^3}{\sum n_i d_i^2} \quad (1)$$

where n_i is the number of clusters with a diameter d_i from >1000 clusters. The values of $\langle d_{TEM} \rangle$ and $\langle d_{chem} \rangle$ are similar for these samples (Table 1), except for the larger Ir clusters; this sample appears to contain some very small Ir clusters that were not detected by TEM when imaging at the magnification level needed to observe the large clusters. Values of $\langle d_{chem} \rangle$ are more reliable in this case, because they include the contributions from all metal clusters present and depend directly on M_s which can adsorb reactants. Consequently, we refer to metal clusters using the sizes derived from chemisorption measurements, $\langle d_{chem} \rangle$. Representative TEM images and cluster size distributions are included in the Supporting Information (Figures S1–S5).

2.3. Catalytic Rate and Selectivity Measurements. Reaction rates were measured using catalysts contained within a packed-bed stainless steel tubular reactor (3/8 in. O.D.) with plug-flow hydrodynamics. The reactor was placed within a three-zone resistively heated furnace and the bed temperature was measured with a type K thermocouple held within a 1/16 in. stainless steel sheath aligned axially within the bed. Catalysts were mixed with additional SiO_2 (Cab-O-Sil HS-5, washed with deionized water and treated in flowing dry air at 793 K for 5 h) in order to avoid axial or radial temperature gradients. Reactor pressures were kept constant using a backpressure regulator (Mity-Mite, model S91XW). The catalyst was treated in flowing H_2 (Praxair, 99.999%) at ambient pressure (50 cm^3 g^{-1} s^{-1}) by heating to 673 at 5 K min^{-1} and holding for 2 h before measuring reaction rates. The molar flow rates and composition of the reactant stream were set using electronic mass flow controllers (Parker, 201). Liquid hydrocarbons (2,3-dimethylbutane, Alfa-Aesar, >99%; 2-methylpentane, Sigma, analytical standard; *n*-hexane, Alfa-Aesar, 99%; *n*-octane, Alfa-Aesar, 99%; toluene, Sigma-Aldrich, anhydrous, >99.8%) were introduced using a high-pressure syringe pump (Isco, 500D). H_2 (Praxair, 99.999%), ethane (5% ethane, 10% Ar, 85% He, Praxair, certified-grade), propane (10% propane, 5% Ar, 85% He, Praxair, certified-grade), *n*-butane (10% *n*-butane, 5% Ar, 85% He, Praxair, certified-grade), and isobutane (1% isobutane, 5% Ar, 94% He, Praxair, certified-grade) flow rates were set by electronic mass flow controllers (Parker, model 201). Transfer lines, before and after the reactor, were maintained at ~423 K to prevent condensation. No reaction products were detected at these conditions in the absence of the metal cluster catalysts, therefore we conclude that hydrogenolysis reactions do not occur on the transfer lines, the walls of the reactor, or on the bare SiO_2 used as a diluent.

The identity and concentrations of hydrocarbons in the reactor effluent were determined by gas chromatography (Agilent GC, 5890) using a methyl silicone capillary column (HP-1, 50 m × 0.32 mm × 1.05 μm) and flame ionization detection. An isoparaffin mixture (Sigma-Aldrich, Isoparaffins Mix, 44586-U) was used to determine retention times and speciation was confirmed by mass spectrometry (Agilent, 5975C). Rates were measured at <10% reactant conversion to ensure that all products were formed in primary reactions and that depletion of reactants did not influence measured rates. Turnover rates are calculated by dividing the conversion of the reactant alkanes by the residence time, which is equal to the moles of M_s divided by the molar flow rate of C atoms from the reactant. These turnover rates are reported as moles of carbon converted per second per mole of M_s ((mol C) (mol M_s·s)$^{-1}$).

3. RESULTS AND DISCUSSION

3.1. Elementary Steps and Rate Equation for C–C Bond Cleavage Reactions. Figure 1 shows hydrogenolysis turnover rates as a function of alkane pressure for ethane and isobutane reactants on Ir, Pt, Rh, and Ru clusters (Figure 1a) and as a function of H_2 pressure for C_2–C_6 *n*-alkanes and isoalkanes on 0.7 nm Ir clusters (Figure 1b). C–C bond cleavage rates are

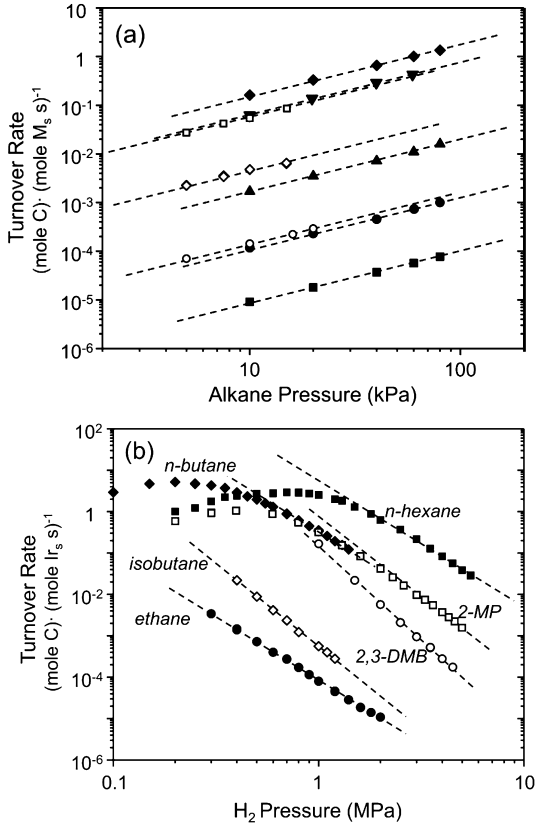

Figure 1. (a) C–C bond cleavage turnover rates (i.e., per exposed metal atom) as a function of alkane pressure on hydrogen-covered metal surfaces for ethane on 0.7 nm Ir (●, 1.0 MPa H_2, 593 K), 7 nm Ir (▼, 1.0 MPa H_2, 593 K, adapted from ref 21), 0.6 nm Pt (■, 1.0 MPa H_2, 653 K), 0.9 nm Rh (▲, 1.0 MPa H_2, 593 K), 1.0 nm Ru (◆, 1.0 MPa H_2, 593 K); and isobutane on 0.7 nm Ir (◇, 1.0 MPa H_2, 593 K), 0.6 nm Pt (○, 1.0 MPa H_2, 653 K), 0.9 nm Rh (□, 1.0 MPa H_2, 593 K). (b) Hydrogenolysis turnover rates as a function of H_2 pressure for ethane (●, 20 kPa), isobutane (◇, 5 kPa), 2,3-dimethylbutane (○, 10 kPa), *n*-butane (◆, 20 kPa), 2-methylpentane (□, 10 kPa), and *n*-hexane (■, 20 kPa) on hydrogen-covered surfaces of 0.7 nm Ir clusters supported on silica, at 593 K. Data for *n*-alkanes adapted from ref 11.

dx.doi.org/10.1021/ja5037429 | J. Am. Chem. Soc. 2014, 136, 9664–9676

shown to be proportional to alkane pressure ($(C_nH_{2n+2})^{1.0\pm0.1}$, Figure 1a) and to depend inversely on H_2 pressure ($(H_2)^{-\lambda}$, Figure 1b). The λ values in this inverse relation reach a constant value at high H_2/C_nH_{2n+2} ratios (>60), but are different for *n*-alkanes ($\lambda = 3.0 \pm 0.2$) and isoalkanes ($\lambda = 3.0-4.5 \pm 0.2$).

Scheme 1 shows a sequence of elementary steps that describe these kinetic effects for isoalkanes and *n*-alkanes, and also for

Scheme 1. Proposed Intermediate Reactions for Hydrogenolysis of Alkanes on Supported Metal Clusters[a]

$$H_2 + 2^* \underset{k_{-H2}}{\overset{k_{H2}}{\rightleftharpoons}} 2\,H(^*) \quad (1.1)$$

$$C_nH_{2n+2} + ^* \underset{k_{-A}}{\overset{k_{A}}{\rightleftharpoons}} C_nH_{2n+2}(^*) \quad (1.2)$$

$$C_nH_{2n+2}(^*) + ^* \underset{k_{-CH,1}}{\overset{k_{CH,1}}{\rightleftharpoons}} C_nH_{2n+1}(^*) + H(^*) \quad (1.3)$$

$$C_nH_{2n+1}(^*) + 2^* \underset{k_{-CH,2}}{\overset{k_{CH,2}}{\rightleftharpoons}} C_nH_{2n}(2^*) + H(^*) \quad (1.4)$$

$$\rightarrow \rightarrow \rightarrow$$

$$C_nH_{2n+2-(y-1)}(\gamma^*) + ^* \underset{k_{-CH,y}}{\overset{k_{CH,y}}{\rightleftharpoons}} C_nH_{2n+2-y}(\gamma^*) + H(^*) \quad (1.5)$$

$$C_nH_{2n+2-y}(\gamma^*) \xrightarrow{k_{CC,y}} C_aH_{a'}(a''^*) + C_bH_{b'}(b''^*) \quad (1.6)$$

$$C_aH_{a'}(a''^*) + xH(^*) \underset{k_{-Ca}}{\overset{k_{Ca}}{\rightleftharpoons}} C_aH_{2a+2} + (a''+x)^* \quad (1.7)$$

[a]* is an unoccupied surface site; $X(n^*)$ denotes an intermediate (X) bound to n sites; $\rightleftharpoons$ denotes a quasi-equilibrated step; k_x and K_x are kinetic and equilibrium constants, respectively, for each reaction; y is the number of H-atoms removed from the alkane to form the reactive intermediate; and γ is the number of sites that bind the reactive intermediate.

ethane[19,30−35] and larger *n*-alkanes;[11,36−38] this sequence and the resulting rate equation are consistent with the measured dependence of isoalkane hydrogenolysis rates on H_2 and isoalkane concentrations reported here. Scheme 1 includes steps for H_2 dissociation (1.1) and for the molecular adsorption of alkanes (C_nH_{2n+2}) (1.2) and their dehydrogenation ($C_nH_{2n+2}(^*)$, where (*) denotes a metal atom) via sequential C−H bond cleavage (1.3−1.5) to form a pool of quasi-equilibrated unsaturated intermediates with y H atoms removed from the C_nH_{2n+2} reactant ($C_nH_{2n+2-y}(\gamma^*)$, where $1 \le y \le 2n+2$ and γ is the number of vicinal surface metal atoms used to bind the intermediate). C−C bonds can cleave in any of these $C_nH_{2n+2-y}(\gamma^*)$ intermediates, which can differ in the number and location of the H atoms removed. H−H and C−H bond dissociation steps (steps 1.1−1.5) are assumed to be quasi-equilibrated, as shown by DFT calculations for ethane hydrogenolysis on Ir[19] and by the prevalent equilibration of isobutane-isobutene and cycloalkane-arene mixtures during hydrogenolysis reactions on Ir, Pt, Ru, and Rh clusters.

Measured hydrogenolysis turnover rates (Figure 1) represent the combined rates of C−C bond cleavage at all positions within the quasi-equilibrated pool of reactive surface intermediates ($C_nH_{2n+2-y}(\gamma^*)$). These intermediates cleave C−C bonds at rates proportional to their respective surface concentrations:

$$r_y = k_{CC,y}[C_nH_{2n+2-y}(\gamma^*)] \quad (2)$$

where $k_{CC,y}$ represents the rate constant for cleaving each specific C−C bond. At high H_2/C_nH_{2n+2} ratios (>60), hydrogenolysis rates depend inversely on H_2 pressure for all isoalkanes (C_4−C_6, Figure 1b) and *n*-alkanes (Figure 1b),[11] because H* reach saturation coverages and become the prevalent adsorbed species (most abundant surface intermediate; MASI). The elementary steps in Scheme 1, taken together with the quasi-equilibrated nature of alkane adsorption and dehydrogenation steps (steps 1.1−1.5),[11,19] lead to the rate equation:

$$r_y = k_{CC,y}\frac{(\prod_{i=1}^{y} K_{CH,i})K_A(C_nH_{2n+2})}{K_{H_2}(H_2)^{\lambda}}[L] \quad (3)$$

Here, K_{H_2} and K_A are the equilibrium constants for H_2 dissociative adsorption and molecular C_nH_{2n+2} adsorption, respectively, and $\prod_{i=1}^{y} K_{CH,i}$ is the product of the equilibrium constants for each of the sequential, quasi-equilibrated C−H bond cleavage steps required to form the reactive intermediate ($C_nH_{2n+2-y}(\gamma^*)$). Equation 3 is consistent with measured hydrogenolysis rates, which are proportional to C_nH_{2n+2} pressure (Figure 1a) and decrease with increasing H_2 pressure (Figure 1b, $\lambda = 3.0-4.5$) at high H_2/C_nH_{2n+2} ratios.

The quasi-equilibrated nature of the elementary steps that cleave (steps 1.1−1.5) and form C−H bonds (step 1.7) renders C−C bond cleavage the sole kinetically relevant step. The apparent rate constant for the cleavage of each C−C bond in a given alkane reactant (k_{app}, where $k_{app} = k_{CC,y}\prod_{i=1}^{y} K_{CH,i}K_A K_{H_2}^{-1}$) depends exponentially on the free energy change ($\Delta G^{\ddagger}$) that occurs when the transition state and λ moles of H_2(g) form via the sequential adsorption and dehydrogenation of the gaseous alkane and the desorption of H* from H*-covered surfaces. Theoretical estimates and experiments have shown that C−C cleavage in ethane occurs on Ir[19] predominantly via one specific intermediate (*CHCH*, α,β-bound to two Ir atoms), because modest differences in free energy barriers, $\Delta G^{\ddagger}$, among transition states for the cleavage of a given C−C bond lead to large concomitant differences in their relative cleavage rates.

3.2. Requirements for Unsaturation and Binding Sites To Form Transition States for C−C Cleavage in Branched, Cyclic, and Linear Alkanes. Figure 2 shows that hydrogenolysis turnover rates when multiplied by $(H_2)^{\lambda}$ become independent of H_2 pressure at high H_2/C_nH_{2n+2} ratios for all alkanes. At these conditions, H* reach saturation coverages and λ reaches constant values (3.0−4.5) for each reactant alkane. Table 2 shows λ values for the cleavage of 22 distinct C−C bonds in linear, branched, and cyclic alkanes on Ir clusters. These λ values (Table 2) are shown in eq 3 to reflect the number of H_2 molecules evolved in forming the reactive C−C bond cleavage intermediate (steps 1.1−1.5). These H_2 molecules are formed from H atoms obtained from the dehydrogenation of the alkane reactant (y, steps 1.2−1.5) and from the desorption of H* from the H*-saturated surface (γ, step 1.1), which is required to bind such reactive species:[11,19]

$$\lambda = \frac{y+\gamma}{2} \quad (4)$$

The intermediates and transition states formed during hydrogenolysis of the various C−C bonds in a given alkane contain C−M bonds (M is a metal surface atom) at each C atom from which an H atom is removed, as shown by experimental[14,39−41] and calculated[13,17,18,42] structures of unsaturated

dx.doi.org/10.1021/ja5037429 | J. Am. Chem. Soc. 2014, 136, 9664−9676

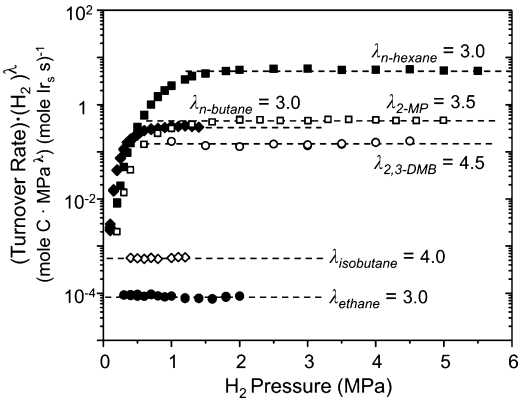

Figure 2. Products of turnover rates and H_2 pressure to the λ power as a function of H_2 pressure for ethane (●), isobutane (◇), 2,3-dimethylbutane (○), *n*-butane (◆), 2-methylpentane (□), and *n*-hexane (■) on hydrogen-covered surfaces of 0.7 nm Ir clusters supported on silica, at 593 K. Values of λ equal the average number of H atoms produced in the gas phase for each C−C bond cleaved for the indicated alkane. Data for *n*-alkanes adapted from ref 11.

hydrocarbons adsorbed on metals at hydrogenolysis temperatures (>500 K). The preference for such structures over adsorbed species containing C═C bonds (or over radical species) reflects the exothermic nature of the conversion of C═C bonds into single C−C bonds with the concomitant formation of two C−M bonds. This reaction is very exothermic [−120 to −60 kJ mol^{-1}; (ΔH_{rxn} = BDE(C═C) − BDE(C−C) − 2BDE(C−M); values of BDE(C−M) from adsorption enthalpies for alkenes and other organic molecules on metals measured calorimetrically[40,43−45] and estimated from theory].[46] On Pt surfaces, experiments[43,45,47] and theory[46] give BDE(^{2}C−Pt) and BDE(^{1}C−Pt) values of 205 and 250 kJ mol^{-1}, respectively, for cyclohexene and ethylene. These values, taken together with the ∼350 kJ mol^{-1} difference between BDE(^{1}C═^{1}C) and BDE(^{1}C−^{1}C) in ethylene and ethane (differences between BDE(C═C) and BDE(C−C) are similar for other hydrocarbons),[48] show that adsorbed hydrocarbons strongly prefer (by ∼100 kJ mol^{-1}) to form C−M bonds at each C atom from which a H atom is removed, instead of replacing such C−H bonds with C═C bonds. The adsorption of a hydrocarbon on H*-saturated surfaces also requires the desorption of H* atoms as H_2(g). Such processes, however, are only mildly endothermic at near-saturation H* coverages (e.g., $\Delta H_{des,H}$ = 17 kJ mol^{-1} at H/Ir$_s$ = 1, on Ir(111) at 593 K).[19] Thus, the formation of C−M bonds from the C═C bond remains exothermic, even after H* desorption.

The equilibrated steps 1.1−1.5 involve elementary reactions that cleave C−H bonds in alkanes and desorb H* to bind the required transition state at vacant sites on H*-saturated surfaces. Such steps form λ H_2 molecules for each transition state, and these λ values are larger for ^{3}C−^{x}C than for ^{2}C−^{2}C and ^{2}C−^{1}C cleavage transition states (Table 2). These data show that the number of H atoms removed from the alkane (y, eq 4) and the number of H* desorbed from the surface (γ, eq 4) depend on the degree of substitution at the C atoms in the cleaved C−C bond. For instance, C_2H_6 hydrogenolysis occurs with a λ value of 3.0 ± 0.2 through a *CHCH* reactive intermediate that has lost two H atoms from each of its two ^{1}C atoms (y = 4)[19] and which requires the desorption of two H* to bind the α,β-bound *CHCH* species (γ = 2, eq 4). On H*-covered Ir clusters, λ values are 3.0 ± 0.2 for all *n*-alkanes (C_2−C_{10});[11] thus, we conclude that reactive

Table 2. λ, $\Delta H^{\ddagger}$, $\Delta S^{\ddagger}$, and $\Delta G^{\ddagger}$ Values for Cleaving Designated C−C Bonds in Linear[11] and Branched Alkanes, and Methylcyclohexane on Hydrogen-Covered Surfaces of 0.7 nm Ir Clusters[a]

Alkane	C-C Bond	λ	$\Delta H^{\ddagger}$ (kJ mol^{-1})	$\Delta S^{\ddagger}$ (J mol^{-1} K^{-1})	$\Delta G^{\ddagger}$ (kJ mol^{-1})
Ethane	H_3C–CH_3	3.0	257	171	156
Propane		3.2	230	164	133
n-Butane		2.9	230	195	114
		2.9	228	181	120
n-Hexane		3.0	213	182	105
		2.8	210	172	108
		2.8	212	167	113
n-Octane		3.0	221	249	73
		3.0	223	254	72
		2.9	218	240	76
		2.9	222	235	83
Isobutane		4.0	256	209	132
2,3-Dimethylbutane		4.3	257	247	111
		4.5	262	268	103
2- Methylpentane		3.4	223	180	116
		3.5	221	185	112
		4.0	240	212	115
		4.2	245	219	115
Methylcyclohexane		2.9	204	173	102
		2.9	211	192	97
		4.0	273	302	94
		4.1	240	253	90

[a]Values of $\Delta G^{\ddagger}$ are determined from ($\Delta G^{\ddagger} = \Delta H^{\ddagger} - T\Delta S^{\ddagger}$) evaluated at 593 K.

intermediates involved in ^{2}C−^{2}C and ^{2}C−^{1}C bond cleavage consist of α,β-bound species with extents of dehydrogenation (and y and γ values) similar to those involved in C_2H_6 hydrogenolysis. For ^{3}C atoms in branched alkanes, however, only one H atom can be removed and one C−M bond formed at any ^{3}C atom in a ^{3}C−^{x}C bond. H atoms must be removed instead from C atoms not involved in the cleaved ^{3}C−^{x}C bond to account for the observed extent of dehydrogenation ($y \geq 5$, Table 2, eq 4). Values of y above three for ^{3}C−^{3}C bonds (or above four for ^{3}C−^{2}C bonds) require H-removal from three or more C atoms; these C atoms must then bind to the surface by forming

dx.doi.org/10.1021/ja5037429 | J. Am. Chem. Soc. 2014, 136, 9664−9676

C−M bonds that require desorption of the H* atoms that previously occupied the binding site.

The measured λ values are larger for ^{3}C−^{x}C bond cleavage in isoalkanes ($4 \leq \lambda \leq 4.5$; Table 2) than for less substituted C−C bonds in *n*-alkanes or isoalkanes (^{2}C−^{2}C, ^{2}C−^{1}C bonds; $\lambda \approx 3$). These larger λ values at more substituted positions indicate that the transition states that mediate ^{3}C−^{x}C activation on H*-covered surfaces require the removal of 8−9 H atoms as H_2(g) (from alkane reactants and surfaces). Such λ values are much larger than those possible by the combined removal of all H atoms in the cleaved ^{3}C−^{x}C bond ($y = 1 + (4 - x)$) and the desorption of two H* to bind two C atoms at surfaces ($\gamma = 2$), which would give λ values of 2.5 for ^{3}C−^{2}C bonds. Consequently, measured λ values for ^{3}C−^{x}C bonds (4.0 or larger; Table 2) indicate that at least one other C atom along the chain must lose H atoms and bind to the surface to form the required transition state. Each bound C atom can reside at an on-top, bridge, or 3-fold site in a manner that preserves its tetrahedral coordination;[41,42,46,49,50] in doing so, each C atom must displace one H*. Thus, reactive intermediates for ^{3}C−^{x}C bond cleavage must occupy a larger number of binding sites ($\gamma \geq 3$) than those for ^{2}C−^{2}C bonds ($\gamma = 2$) because at least three C atoms are dehydrogenated.

The independent values of the parameters y and γ cannot be discerned from experiments alone, because they appear as their sum in the rate equation (i.e., as λ in eq 3). The stoichiometric arguments above, however, provide a way to estimate y and γ for ^{3}C−^{x}C cleavage transition states. Rate data show that 4−4.5 H_2(g) form with each transition state (i.e., $8 \leq (y + \gamma) \leq 9$; Table 2, eq 4), and bond order conservation requires that the number of C atoms coordinated to the surface must be equal to or less than the number of H atoms lost from the alkane by dehydrogenation ($\gamma \leq y$). This reasoning shows that for all ^{3}C−^{x}C bonds studied here (Table 2), γ values range from 3 to 4 and y values range from 4 to 5.

Plausible transition-state structures consistent with these γ and y values and with measured λ values for each of the C−C bonds (Table 2) are shown in Figure 3. (The adsorbate structures shown in Figure 3 represent schematic depictions of possible transition-state structures and were not derived from theoretical calculations.) The cleavage of the central ^{2}C−^{2}C bond in *n*-hexane ($y = 4$; $\gamma = 2$; Figure 3a) is representative of the most stable transition state for cleavage of ^{2}C−^{2}C, ^{2}C−^{1}C, and ^{1}C−^{1}C bonds. In the case of propane, for example, theoretical treatments[51] have confirmed that four H atoms are removed to form an α,β-bound complex in which the ^{2}C−^{1}C bond cleaves in a step that is favored over further hydrogenation by a difference in H_{act} larger than 14 kJ mol^{-1}.[51] The formation of this α,β-bound intermediate and subsequent C−C bond cleavage are similar to the steps found for ethane,[19] because in both cases the ^{1}C−^{x}C bond weakens (H_{act} decreases) as the C atoms involved form additional C−M bonds with the surface. These conclusions are consistent with molecular orbital descriptions of covalent bonding at surfaces,[52] in which elementary steps that form C−M bonds bind the reactive intermediate increasingly tightly as the C atom coordinates first at an on-top site (C−M), then at a bridge site (C═M), and finally at a 3-fold site (C≡M). Quantum chemical calculations indicate that as the C atoms move to occupy higher coordination sites, the extent of electron donation to the surface and back-donation to antibonding C−C orbitals increase and thus weaken the C−C bond.[53]

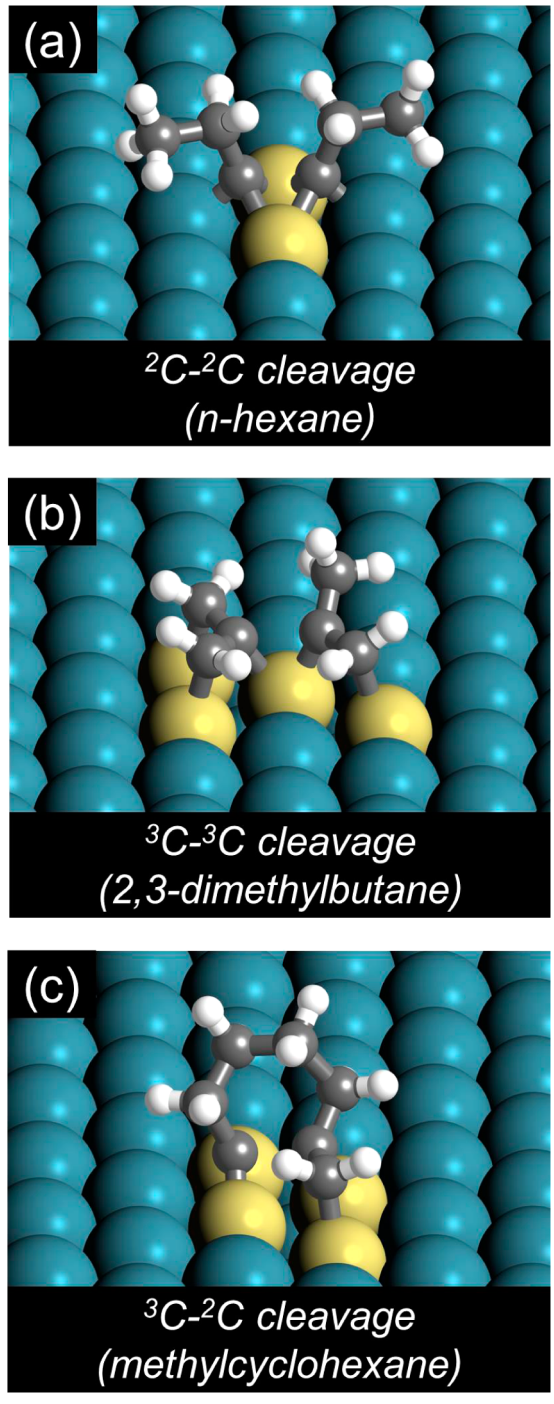

Figure 3. Schematic depictions of potential transition states for cleaving C−C bonds in alkane-derived intermediates, based on measured λ values. (a) α,β-adsorbed structure that cleaves the central C−C bond in *n*-hexane ($y = 4$, $\gamma = 2$; where y is the number of H atoms removed from the alkane to form the intermediate; and γ is the number of sites needed to bind the intermediate); (b) a penta-adsorbed structure that cleave the central ^{3}C−^{3}C bond in 2,3-dimethylbutane ($y = 5$, $\gamma = 4$); (c) α,β,γ-adsorbed structure to cleave the ^{3}C−^{2}C bond in methylcyclohexane ($y = 4$, $\gamma = 4$). These structures are drawn on the basis of principles of bond order conservation and reported conformations of hydrocarbons adsorbed on metal surfaces.[24,16−18,23,46]

^{3}C atoms, however, can form only a single C−M bond, which limits the extent to which such higher surface coordination can weaken ^{3}C−^{x}C bonds. Binding C atoms other than those in the ^{3}C−^{x}C bond at surfaces will influence H_{act} for ^{3}C−^{x}C cleavage

dx.doi.org/10.1021/ja5037429 | J. Am. Chem. Soc. 2014, 136, 9664−9676

only weakly, because electron-donation and back-donation occurs predominantly near the bound C atoms.[53] As a result, $^3C-^xC$ bond cleavage occurs within a transition state different in structure from the α,β-bound transition states that cleave $^2C-^2C$ bonds. The cleavage of the $^3C-^3C$ bond in 2,3-dimethylbutane ($y = 5$, $\gamma = 4$; Figure 3b) and of the $^3C-^2C$ bond within the methylcyclohexane ring ($y = 4$, $\gamma = 4$; Figure 3c) occur via structures bound through three or more C atoms; $^3C-^xC$ bond cleavage specifically occurs via α,β,γ- or $\alpha,\beta,\gamma,\delta$-bound species. Density functional calculations show that the $^3C-^1C$ bonds in isobutane cleave via α,β,γ- or $\alpha,\beta,\gamma,\delta$-bound transition states,[51] because H_{act} for C−H bond cleavage and formation are more than 27 kJ mol^{-1} smaller than for $^3C-^1C$ bond cleavage up to the point when five or more H atoms are lost and three or more C atoms bind to the surface. These highly dehydrogenated transition states form even though the elementary steps involved are endothermic and become more so as the extent of dehydrogenation increases.[19] $^3C-^xC$ bond cleavage occurs in such structure because their $\Delta G^{\ddagger}$ values are less than those for other transition-state structures (such as metallacycles or α,β-bound complexes) and this shows that the unfavorable enthalpy of formation for α,β,γ- or $\alpha,\beta,\gamma,\delta$-bound transition states is compensated by large and positive $\Delta S^{\ddagger}$. Next, we describe evidence for the need for such unsaturated intermediates and multiple surface attachments and for the kinetic consequences of the entropy gains associated with the H_2 molecules evolved upon formation of these transition states.

3.3. Carbon−Carbon Bond Cleavage Transition-State Structures and Activation Enthalpies ($\Delta H^{\ddagger}$) and Entropies ($\Delta S^{\ddagger}$). The quasi-equilibrated nature of steps 1.1−1.5 (Scheme 1) and the thermodynamic basis of all formalisms based on transition-state theory require that C−C bond cleavage transition states be also in equilibrium with gaseous alkane reactants (C_nH_{2n+2}) and H_2 and with all intervening unsaturated intermediates. The lumping of all such equilibrated steps leads to the stoichiometric reaction:

$$C_nH_{2n+2} + \gamma\, H(*) \overset{K'^{\ddagger}}{\rightleftharpoons} C_nH_{2n+2-y}(\gamma^*)^{\ddagger} + \lambda H_2 \qquad (5)$$

on H*-saturated surfaces. Here, $K'^{\ddagger}$ represents the equilibrium constant for the formation of the transition state ($C_nH_{2n+2-y}(\gamma^*)^{\ddagger}$) and of λ gaseous H_2 molecules (where $\lambda = (\gamma + y)/2$). Scheme 2 depicts a thermochemical cycle for the formation of these transition states (for $^2C-^2C$ bond cleavage in alkanes with stoichiometry $R_1(H_2C)(CH_2)R_2$; with values of $y = 4$ and $\gamma = 2$ based on analogy with *n*-alkanes[11] and C_2H_6[19]). This cycle consists of hypothetical steps chosen because their thermodynamic properties are available[54] or amenable to theoretical estimates.[19] These steps and the corresponding free energy changes include (i) dehydrogenation of the alkane in the gas phase to form a species with the H-content of the reactive intermediate (ΔG_D); (ii) recombinative desorption of H* atoms to form the vacancies required for binding the intermediate (ΔG_H); (iii) adsorption of the intermediate on the surface (ΔG_A); and (iv) formation of the C−C cleavage transition state (ΔG_R). The Gibbs free energy of activation ($\Delta G^{\ddagger}$) on H*-covered surfaces becomes

$$\Delta G^{\ddagger} = G^{\ddagger} + \lambda G_{H_2} - \gamma G_{H^*} - G_{C_nH_{2n+2}} \qquad (6)$$

Here, $G^{\ddagger}$ is the transition-state free energy, G_{H_2} and $G_{C_nH_{2n+2}}$ are the free energies of H_2(g) and C_nH_{2n+2}(g), respectively, and G_{H^*} is the free energy of chemisorbed H*.[11]

Scheme 2. Thermochemical Cycle Accounting for Free Energy Changes for the Reaction Sequence, Shown in Scheme 1, which Forms Transition States for C−C Bond Cleavage on H*-Covered Surfaces, Depicted Here for $^2C-^2C$ Bond Cleavage in the Alkane $R_1(H_2C)(CH_2)R_2$[a]

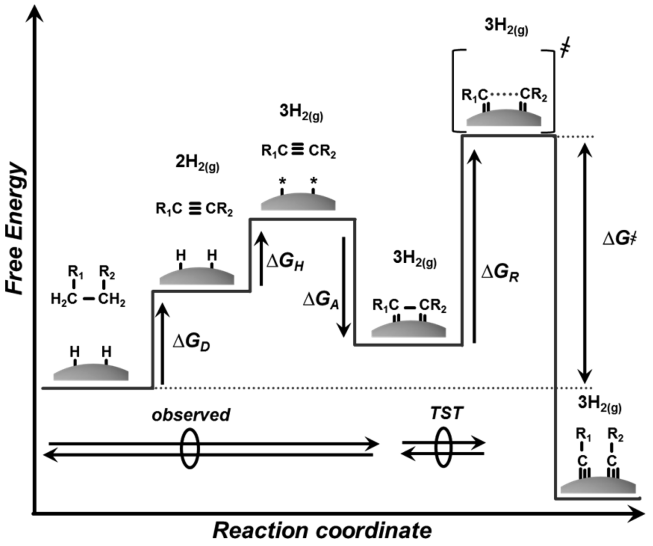

[a]Free energy changes are shown for lumped steps that dehydrogenate the alkane (ΔG_D), desorb hydrogen (ΔG_H), adsorb the dehydrogenated hydrocarbon (ΔG_A), and rupture the C−C bond (ΔG_R). (⟷ denotes groups of quasi-equilibrated steps that are observed directly or implied by transition-state theory (TST); and the moles of gas-phase H_2 indicated are cumulative along the reaction coordinate). Measured activation free energies, $\Delta G^{\ddagger}$, equal the sum of free energy changes for all preceding steps and depend, in part, on the free energy of the transition state ($G^{\ddagger}$) and the gaseous H_2 (G_{H_2}) that is produced in quasi-equilibrated steps that form the transition state (eq 6).

Equation 6 shows that $\Delta G^{\ddagger}$ values for the cleavage of a given C−C bond depend only on the stability of the reactants (C_nH_{2n+2}(g); H*) and products ($C_nH_{2n+2-y}(\gamma^*)^{\ddagger}$, H_2(g)) in eq 5 and on the values of λ and γ for the transition state; therefore, the identity and free energy of any intervening species are not relevant to the dynamics of C−C cleavage. The combination of eq 4 and eq 6 shows that $\Delta G^{\ddagger}$ depends on the individual values of y and γ as

$$\Delta G^{\ddagger} = G^{\ddagger} + \frac{y}{2}G_{H_2} + \gamma\left(\frac{G_{H_2}}{2} - G_{H^*}\right) - G_{C_nH_{2n+2}} \qquad (7)$$

This relationship and the negative values of G_{H_2} and G_{H^*} at typical hydrogenolysis temperatures (e.g., at 500 K, $G_{H_2} = -78$ kJ mol^{-1},[55] and $G_{H^*} = -27$ kJ mol^{-1} at H*/Ir$_s$ = 1)[19] show that $\Delta G^{\ddagger}$ values for cleaving a specific C−C bond tend to decrease as y and γ increase. Thus, eqs 6 and 7 provide the basis for understanding the effects of substitution on C−C cleavage rates and for interpreting differences between $\Delta G^{\ddagger}$ values for cleaving $^3C-^xC$ bonds and those for C−C bonds involving less substituted C atoms.

The hydrogenolysis rate equations (eqs 1−3) can be recast in terms of $\Delta G^{\ddagger}$ (eq 6) and ultimately in terms of $\Delta H^{\ddagger}$ and $\Delta S^{\ddagger}$ (using $G = H - TS$):

dx.doi.org/10.1021/ja5037429 | J. Am. Chem. Soc. 2014, 136, 9664−9676

$$\frac{r}{[L]} = \frac{k_B T}{h} K^{\ddagger} \frac{(C_nH_{2n+2})}{(H_2)^{\lambda}} = \frac{k_B T}{h} e^{\Delta S^{\ddagger}/R} e^{-\Delta H^{\ddagger}/RT} \frac{(C_nH_{2n+2})}{(H_2)^{\lambda}} \quad (8)$$

Here, k_B and h are the Boltzmann and Planck constants, respectively, and $K^{\ddagger}$ is the transition-state equilibrium constant (eq 5). The latter is estimated from statistical mechanics formalisms, using partition functions that exclude the symmetric C−C bond stretch along the reaction coordinate for the transition state.[11] The measured effects of temperature on hydrogenolysis rates can then be used to determine $\Delta H^{\ddagger}$ and $\Delta S^{\ddagger}$ values for each alkane at each distinct C−C position, after normalization by the number of C−C bonds of each type. These $\Delta H^{\ddagger}$ and $\Delta S^{\ddagger}$ values represent the additive enthalpic and entropic contributions from each step in the thermochemical cycle (Scheme 2) for the cleavage of each distinct C−C bond in each alkane reactant.

Figure 4 shows the measured equilibrium constants ($K^{\ddagger}$) for the formation of transition states that mediate the cleavage of

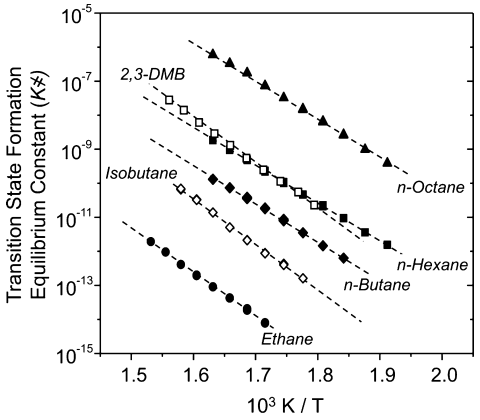

Figure 4. Eyring−Polanyi plot of $K^{\ddagger}$, the equilibrium constant for the formation of transition states with respect to the gas-phase alkane reactant and the H*-covered surface (eq 5), as a function of inverse temperature for the conversion of ethane (●), isobutane (◇), *n*-butane (◆), *n*-hexane (■), 2,3-dimethylbutane (□), and *n*-octane (▲) on hydrogen-covered surfaces of 0.7 nm Ir clusters supported on silica. $K^{\ddagger}$ values for *n*-alkanes[11] are shown for comparison to isoalkanes.

^{3}C−^{1}C bonds in isobutane and of ^{3}C−^{3}C and ^{3}C−^{1}C bonds in 2,3-dimethylbutane, as well as C−C bonds with less substituted C atoms (^{2}C−^{2}C and ^{2}C−^{1}C bond cleavage in *n*-alkanes, C_2−C_8)[11] on H*-covered Ir clusters as a function of reciprocal temperature. These data, as well as the $K^{\ddagger}$ values for the cleavage of each distinct C−C bond in these alkanes and 2-methylpentane (2-MP) and methylcyclohexane (MCH) (not shown in Figure 4), lead to the $\Delta H^{\ddagger}$ and $\Delta S^{\ddagger}$ values reported for these reactions in Table 2.

$\Delta H^{\ddagger}$ values reflect differences between the enthalpy of products (the transition state, $H^{\ddagger}$, and λ molecules of gas-phase H_2, λH_{H_2}) and reactants (gaseous alkanes, $H_{C_nH_{2n+2}}$, and γ chemisorbed H atoms, γH_{H^*}) in eq 5:

$$\Delta H^{\ddagger} = H^{\ddagger} + \lambda H_{H_2} - \gamma H_{H^*} - H_{C_nH_{2n+2}} \quad (9)$$

On H*-covered metal clusters, $\Delta H^{\ddagger}$ depends on the strength of the C−C bond [BDE(C−C), accounting in part for differences between $H^{\ddagger}$ and $H_{C_nH_{2n+2}}$], on the number of H* desorbed to bind the transition state (γ), and on the number of H_2(g) molecules formed from desorption and from dehydrogenation of alkane reactants to form the unsaturated reactive intermediate (λ). $\Delta H^{\ddagger}$ values range from 177 to 262 kJ mol^{-1}; they are larger for stronger C−C bonds (e.g., $\Delta H^{\ddagger}$ = 257 kJ mol^{-1} for ^{1}C−^{1}C bonds, where BDE(^{1}C−^{1}C) is 378 kJ mol^{-1})[10] than for weaker C−C bonds (e.g., $\Delta H^{\ddagger}$ = 230 kJ mol^{-1} for ^{2}C−^{2}C bonds, where BDE(^{2}C−^{2}C) is 344 kJ mol^{-1}),[10] when such comparisons are restricted to C−C bonds with only ^{2}C- and ^{1}C-atoms. $\Delta H^{\ddagger}$ values for all C−C bonds within a given *n*-alkane reactant are similar (±2 kJ mol^{-1}) on 0.7 nm Ir.[11] The $\Delta H^{\ddagger}$ differences among different *n*-alkanes, however, are proportional to the differences in their respective BDE(C−C) averaged over all C−C bonds in each given *n*-alkane.[11] Thus, *n*-alkanes with larger average BDE(C−C) values cleave C−C bonds with larger $\Delta H^{\ddagger}$ values, suggesting that $\Delta H^{\ddagger}$ differences among ^{2}C−^{2}C, ^{2}C−^{1}C, and ^{1}C−^{1}C bonds predominantly reflect their respective BDE(C−C) values.

Similar trends are not evident when these comparisons are extended to include C−C bonds containing ^{3}C atoms. $\Delta H^{\ddagger}$ values for ^{3}C−^{x}C bonds are larger than for ^{2}C−^{2}C or ^{2}C−^{1}C bonds by 20−30 kJ mol^{-1} (Table 2), even though their BDE(^{3}C−^{x}C) values are actually smaller (by 2−5 kJ mol^{-1}) than for ^{2}C−^{2}C and ^{2}C−^{1}C bonds.[10] In fact, the $\Delta H^{\ddagger}$ value for the weaker ^{3}C−^{3}C bond in 2,3-DMB ($\Delta H^{\ddagger}$ = 257 kJ mol^{-1}; BDE(^{3}C−^{3}C) = 330 J mol^{-1} K^{-1})[10] is nearly the same as for the much stronger (by 48 kJ mol^{-1})[10] ^{1}C−^{1}C bond in ethane (Table 2). These data indicate that methyl substitution leads to higher $\Delta H^{\ddagger}$ values through effect(s) unrelated to the strength of the reacting C−C bond (i.e., BDE(C−C)).

C−C bond cleavage occurs in alkane-derived intermediates when the activation free energy (G_{act}) to break the C−C bond becomes smaller than that for additional C−H bond ruptures.[19] The mechanistic interpretation of eq 4 indicates that λ differences among C−C bonds reflect concomitant differences in the combined number of C−H bonds and M−H bonds cleaved; these λ values are much larger for cleaving ^{3}C−^{x}C bonds (λ = 4−4.5, and $4 \le y \le 5$) than ^{2}C−^{2}C bonds (λ = 3, y = 4). Thus, G_{act} values for ^{3}C−^{x}C bond rupture remain higher than for C−H bond rupture until 2−3 additional H atoms are removed from reactants and surfaces compared with the case of ^{2}C−^{2}C bond cleavage. The loss of more hydrogen from the reactant and from the surface (as additional C−M bonds form) causes ^{3}C−^{x}C bonds to cleave with larger $\Delta H^{\ddagger}$ than ^{2}C−^{2}C bonds, because these elementary steps are endothermic (i.e., BDE(C−H) + BDE(M−H) > BDE(C−M))[19,40,43−46] and additive (eqs 5, 9). Thus, sequential steps that dehydrogenate and bind reactants at vacancies formed on H*-covered surfaces are endothermic (as shown by DFT calculations for ethane hydrogenolysis)[19] and become increasingly so as the number of C−H bonds (y) and M−H bonds broken (γ) increase. Higher $\Delta H^{\ddagger}$ values for ^{3}C−^{x}C cleavage (relative to ^{2}C−^{2}C cleavage and measured with respect to the C_nH_{2n+2}(g) and γ H* (eq 5)) are consistent with transition states with larger λ values than for ^{2}C−^{2}C or ^{2}C−^{1}C cleavage (Table 2).

^{3}C−^{x}C cleavage transition states form a larger number of H_2(g) molecules than for ^{2}C−^{2}C cleavage, because at least three C atoms dehydrogenate and bind to the surface before bond cleavage becomes more favorable than additional dehydrogenation events. These λ and $\Delta H^{\ddagger}$ values show that ^{3}C−^{x}C bond cleavage involves the formation of more H_2(g) than for ^{2}C−^{2}C bonds, possibly because ^{3}C atoms are unable to form more than a single C−M bond, thus preventing their migration to higher

dx.doi.org/10.1021/ja5037429 | J. Am. Chem. Soc. 2014, 136, 9664−9676

coordination sites, where greater orbital overlap and electron donation and back-donation to and from the surface would decrease H_{act} values for such ^{3}C−^{x}C bonds.[53] We have recently shown that the H_{act} values for cleavage of the C−C bond in ethane decrease as the reactive intermediate dehydrogenates,[19] consistent with the importance of high coordination binding sites proposed here, and these considerations are being more rigorously explored in isoalkanes using DFT methods.[51]

The large $\Delta H^{\ddagger}$ values for alkane hydrogenolysis (Table 2) seem incongruous at first glance in view of the modest temperatures required for such reactions (500−650 K). These hydrogenolysis rates reflect large and positive activation entropies ($\Delta S^{\ddagger}$ = 164−268 J mol^{-1} K^{-1}, Table 2) brought forth by the release of λ moles of H_2 upon formation of the C−C bond cleavage transition states from their relevant precursors:

$$\Delta S^{\ddagger} = S^{\ddagger} + \lambda S_{H_2} - \gamma S_{H^*} - S_{C_nH_{2n+2}} \quad (10)$$

Here, the entropies of the species are defined as in the case of enthalpies (eq 9) and correspond to the species shown in Scheme 2. The values of S_{H_2} (140−130 J mol^{-1} K^{-1}, 1−4 MPa H_2, respectively) and $S_{C_nH_{2n+2}}$ (290−652 J mol^{-1} K^{-1} for gaseous C_2H_6 to n-C_8H_{18}, 5−20 kPa, 593 K) can be estimated from partition functions for three-dimensional ideal gases, using the formalism of statistical mechanics.[11,55,56] S_{H^*} values on H*-saturated surfaces (H*/M$_s$ = 1) at 593 K can be estimated from treatments of two-dimensional ideal gases (35 J mol^{-1} K^{-1}).[56] These estimates and measured $\Delta S^{\ddagger}$ values can be used to determine $S^{\ddagger}$ values, and these values can then be compared with estimates for proposed C−C bond cleavage transition states obtained from statistical mechanics to assess the plausibility of these structures.

Previous studies have shown that $S^{\ddagger}$ values for cleaving C−C bonds in n-alkanes can be estimated from partition functions that consider frustrated two-dimensional translations ($S^{\ddagger}_{2D,trans}$), intramolecular vibrations($S^{\ddagger}_{vib}$), rotational conformations about each C−C bond ($S^{\ddagger}_{conf}$), and rigid rotations of the alkyl-chains attached to the C atoms at the C−C bond being cleaved ($S^{\ddagger}_{1D,rot}$).[11] ($S^{\ddagger}_{vib}$ is assumed to be those in the gas-phase analogues with the exception of the C−C bond vibration corresponding to the reaction coordinate and the replacement of four C−H bonds with C−M bonds.) On Ir clusters, C−C bonds cleave at every position within n-alkanes with identical λ (λ = 3.0 ± 0.2) and γ (γ = 2) values.[11] Differences in $\Delta S^{\ddagger}$ among different C−C bonds in n-alkanes (Table 2), therefore, solely reflect $S^{\ddagger}_{1D,rot}$ differences, which depend, in turn, only on the length of each of the two alkyl rigid rotors[11] (shown as propyls in Figure 3a). Estimates for $S^{\ddagger}_{1D,rot}$ in n-alkanes are very reliable, because transitions states for ^{2}C−^{2}C and ^{2}C−^{1}C bond cleavage are α,β-coordinated at surfaces through the two C atoms in the bond that breaks and the length of the alkyl rigid rotors in these structures is rigorously and fully defined by the position of the cleaved C−C bond. The $S^{\ddagger}_{1D,rot}$ values for transition states that cleave ^{3}C−^{x}C bonds are less clearly defined, because other C atoms, at locations unknown, also bind to the surface, making the length of the alkyl rotors uncertain.

$\Delta S^{\ddagger}$ values for ^{3}C−^{x}C cleavage are larger than for ^{2}C−^{2}C or ^{2}C−^{1}C bond cleavage (Table 2), because of the larger number of H_2(g) molecules evolved in forming the transition state. The transition states that mediate ^{3}C−^{x}C cleavage, however, have less entropy than for ^{2}C−^{2}C or ^{2}C−^{1}C cleavage, because they coordinate to surfaces through three or more C atoms (e.g., α,β,γ- bound; Figure 3b,c),[17,18,20] in contrast to the two C atoms that bind in the α,β-complexes that cleave ^{2}C−^{2}C and ^{2}C−^{1}C bonds (Figure 3a). More specifically, the $S^{\ddagger}$ values for ^{3}C−^{x}C bond cleavage transition states are smaller than for ^{2}C−^{2}C and ^{2}C−^{1}C cleavage in alkanes of a given carbon number because the additional attachments shorten the alkyl rigid rotors (Figure 3a), thus making $S^{\ddagger}_{1D,rot}$ values smaller than those for α,β-bound transition states.[11] For example, the transition-state entropy for cleaving the central C−C bond in n-hexane (Figure 3a) decreases by 12−30 J mol^{-1} K^{-1} for each additional C atom that binds to the metal surface (see Supporting Information). Specifically, $S^{\ddagger}_{1D,rot}$ will decrease by 12 J mol^{-1} K^{-1} if a ^{2}C−M bond forms adjacent to the α,β-coordinated C atoms shown in Figure 3a; and $S^{\ddagger}_{1D,rot}$ will decrease by ∼30 J mol^{-1} K^{-1} if a ^{1}C−M bond forms at the ^{1}C atom at the end of the propyl chain (Figure 3a). These additional C−M bonds also increase surface diffusion barriers (E_d) and thus the frequency of frustrated translational modes, leading to a concomitant decrease in mobility and in $S^{\ddagger}_{2D,trans}$ values. Losses in $S^{\ddagger}_{2D,trans}$ (<5 J mol^{-1} K^{-1} at 593 K, assuming that E_d doubles) are much smaller, however, than the concurrent losses of rotational freedom reflected in $S^{\ddagger}_{1D,rot}$ values and caused by the binding of more C atoms to the surface (Supporting Information). Taken together, these rotational and translational entropy differences lead to estimates for $S^{\ddagger}$ values (from statistical mechanics) for ^{3}C−^{x}C bond cleavage in C_4 (i.e., isobutane) that are 20−50 J mol^{-1} K^{-1} smaller than for n-butane (see Supporting Information for detailed discussion of the range of these differences). Similarly, $S^{\ddagger}$ estimates for ^{3}C−^{x}C bond cleavage in C_6 isoalkanes (i.e., 2-methylpentane, 2,3-dimethyl-butane) are 30−70 J mol^{-1} K^{-1} smaller than for n-hexane,[11] based on their y and γ values and their binding configurations (Figure 3a,b). The significant uncertainty in predicted $S^{\ddagger}$ values (30−40 J mol^{-1} K^{-1}) reflects the indeterminate number and location (along the chain) of the C−M bonds formed at each transition state, which must be known for more rigorous $S^{\ddagger}_{1D,rot}$ estimates. We conclude that $\Delta S^{\ddagger}$ values are larger for ^{3}C−^{x}C than for ^{2}C−^{2}C, ^{2}C−^{1}C, and ^{1}C−^{1}C cleavage (Table 2) because of their concomitantly larger λ values. The formation of 1−1.5 more H_2(g) for ^{3}C−^{x}C cleavage (over that for less substituted C−C bonds; eq 10; Table 2) give larger entropy gains (130−195 J mol^{-1} K^{-1}, for S_{H_2} =130 J mol^{-1} K^{-1}), which dominate over the $S^{\ddagger}$ losses (20−70 J mol^{-1} K^{-1}) caused by the additional surface attachments through C−M bonds.

Figure 5 shows $S^{\ddagger}$ estimates for C−C bond cleavage in isoalkanes and n-alkanes from statistical mechanics treatments, together with measured $S^{\ddagger}$ values obtained from $\Delta S^{\ddagger}$ values (Table 2) and calculated using eq 10 [with $(y-1) < \gamma \leq y$ (eq 4) for isoalkanes; values for n-alkanes from ref 11]. The predicted $S^{\ddagger}$ value for each ^{3}C−^{x}C bond represents the average $S^{\ddagger}$ values for the various transition-state structures with y and γ values consistent with measured λ values (Table 2); the uncertainty intervals in the abscissa values reflect the range of $S^{\ddagger}$ values obtained for all such possible transition-state structures. The value of γ (the number of H* displaced to accommodate the transition state) cannot be measured independently of y (the number of H atoms removed from the alkane) and thus represents the most significant uncertainty in measured $S^{\ddagger}$ values. Bond order conservation considerations indicate that the number of adsorption sites (γ) needed to bind the transition state would always be smaller than or equal to the number of H atoms removed from the alkane, therefore, we do not consider the relationship $y < \gamma \leq (y+1)$ as a possibility. Experimental and predicted $S^{\ddagger}$ values agree well (Figure 5; 1.03 ± 0.02 correlation

dx.doi.org/10.1021/ja5037429 | J. Am. Chem. Soc. 2014, 136, 9664−9676

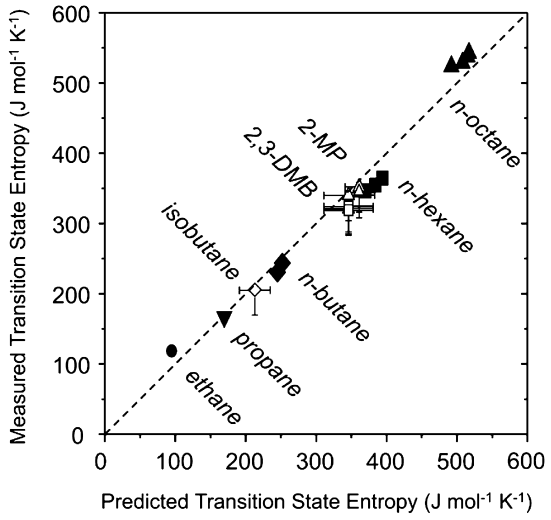

Figure 5. Comparison between predicted and measured transition-state entropies for complexes that cleave C−C bonds in isoalkanes (empty symbols) and *n*-alkanes (filled symbols, adapted from ref 11). (Predicted $S^{\ddagger}$ values for isoalkanes are assumed to possess one-half the average rotational entropy ($S_{1D,rot}{}^{\ddagger}$) of the *n*-alkane with identical number of carbon atoms. Asymmetric error bars reflect differences between plausible transition-state structures. The value of γ may be overestimated by one (vertical uncertainty), and transition states may possess smaller or larger $S_{1D,rot}{}^{\ddagger}$ than assumed here (horizontal uncertainty), because the position of C−M bonds within the transition state are uncertain.) Values from H*-covered surfaces of 0.7 nm Ir clusters, 593 K (ethane (●), propane (▼), isobutane (◇), *n*-butane (◆), 2,3-dimethylbutane (□), 2-methylpentane (Δ), *n*-hexane (■), and *n*-octane (▲)). Alkanes that contain distinguishable C−C bonds are represented by multiple points showing predicted and measured transition-state entropies for C−C bonds rupture.

slope; -17 ± 11 J mol^{-1} K^{-1} intercept), indicating that transition states for ^{3}C−^{x}C bond cleavage in all isoalkanes have much less entropy than their *n*-alkane analogues because of the smaller $S^{\ddagger}_{1D,rot}$ values for the α,β,γ-bound complexes (e.g., measured $S^{\ddagger}$ is 204 J mol^{-1} K^{-1} for the ^{3}C−^{1}C bond of isobutane and 231 and 244 J mol^{-1} K^{-1} for ^{2}C−^{1}C and ^{2}C−^{2}C bonds, respectively, of *n*-butane, Figure 5). The agreement between experimental and predicted $S^{\ddagger}$ values (Figure 5) provides compelling evidence for the reasonable nature of the proposed mechanism and transition-state structures for the cleavage of ^{3}C−^{x}C bonds (i.e., three of more C atoms coordinated to the metal surface, Figure 3b).

3.4. Location of C−C Bond Cleavage within Isoalkanes.

The different transition-state structures that cause the distinct reactivity of ^{x}C−^{y}C bonds in linear and branched alkanes also account for the location of C−C bond cleavage along the chain of a given isoalkane. Figure 6 shows that turnover rates for C−C cleavage at unsubstituted (^{2}C−^{2}C and ^{2}C−^{1}C bonds) and substituted (^{3}C−^{x}C bonds) positions in 2-methylpentane (2-MP) depend differently on H_2 pressure (10 kPa 2-MP, 0.2−5.5 MPa H_2, 593 K). Their different λ values (Table 2) reflect different extents of dehydrogenation and numbers of surface attachments for the transition states that cleave these two types of C−C bonds in 2-MP. We define χ as the ratio of C−C cleavage rates at unsubstituted (^{2}C−^{2}C, ^{2}C−^{1}C) and substituted (^{3}C−^{x}C) positions:

$$\chi = \frac{r_{^{2}C-^{2}C} + r_{^{2}C-^{1}C}}{r_{^{3}C-^{x}C}} \qquad (11)$$

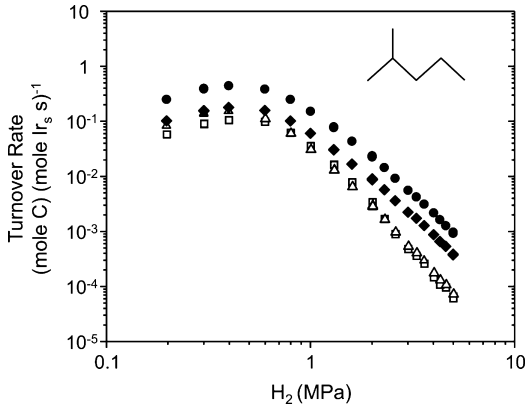

Figure 6. Turnover rates for hydrogenolysis of 2-methylpentane (2-MP) via cleavage of ^{2}C−^{2}C (●), ^{2}C−^{1}C (◆), ^{3}C−^{2}C (Δ), and ^{3}C−^{1}C (□) bonds (0.7 nm Ir clusters, 10 kPa 2-MP, 593 K).

Here, each $r_{^{x}C-^{y}C}$ represents the rate of ^{x}C−^{y}C bond cleavage per ^{x}C−^{y}C bond of a given type in the alkane reactant. For 2-MP, these χ values increase with increasing H_2 pressure (Figure 7),

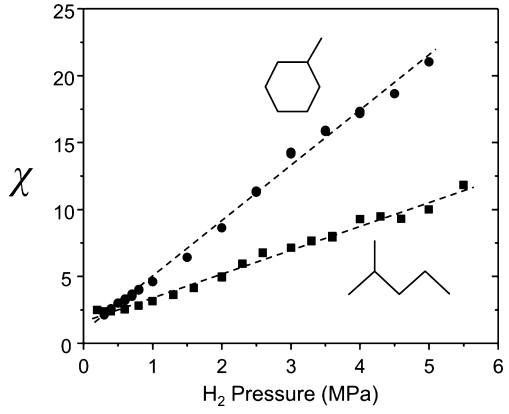

Figure 7. Change in χ, the ratio of the rate of C−C bond cleavage at unsubstituted (^{2}C−^{2}C, ^{2}C−^{1}C) positions to that at substituted positions (^{3}C−^{2}C, ^{3}C−^{1}C), for 2-MP (■, 593 K) and MCH (●, 543 K) as a function of H_2 pressure at 10 kPa alkane pressure, 0.7 nm Ir clusters.

because the concentration of ^{3}C−^{x}C cleavage transition states (from quasi-equilibrated adsorption and dehydrogenation of alkane reactants (eq 5)) decreases more sensitively with H_2 pressure (eq 8, where λ = 4−4.5) than for those involved in ^{2}C−^{2}C and ^{2}C−^{1}C cleavage events (eq 8, where λ = 3−3.5). As a result, the selectivity to branched alkanes among hydrogenolysis products (isobutane, 2-methylbutane) increases with increasing H_2 pressure. In contrast, hydrogenolysis of 2,3-dimethylbutane gives ^{3}C−^{3}C to ^{3}C−^{1}C cleavage rate ratios that do not depend on H_2 pressure or temperature (Figures S7 and S8, Supporting Information). Thus, the differences between λ and $\Delta H^{\ddagger}$ values among ^{3}C−^{x}C bonds are insensitive to the substitution of the second C atom (i.e., the value of *x*; Table 2). Figure 8 shows that χ values for 2-MP increase with decreasing temperature (10 kPa 2-MP, 4.0 MPa H_2, 553−617 K, 0.7 nm Ir clusters), because $\Delta H^{\ddagger}$ values for ^{3}C−^{x}C cleavage in 2-MP are larger than for ^{2}C−^{2}C or ^{2}C−^{1}C cleavage (by 20−25 kJ mol^{-1}; Table 2). These differences between $\Delta H^{\ddagger}$ for ^{3}C−^{x}C and ^{2}C−^{2}C or ^{2}C−^{1}C bonds reflect the greater extent of dehydrogenation (*y*) and the larger number of C atoms bound at surfaces (γ) in the transition states for cleavage of ^{3}C−^{x}C compared to those that cleave ^{2}C−^{2}C or ^{2}C−^{1}C bonds.

dx.doi.org/10.1021/ja5037429 | J. Am. Chem. Soc. 2014, 136, 9664−9676

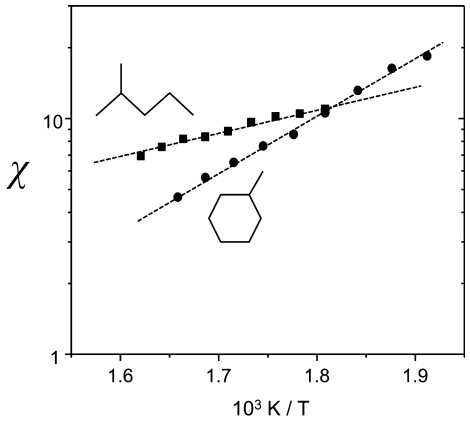

Figure 8. Values of χ, the ratio of the rate of C−C bond cleavage at unsubstituted (^{2}C−^{2}C, ^{2}C−^{1}C) positions to that at substituted positions (^{3}C−^{2}C, ^{3}C−^{1}C), for 2-MP (■, 4.0 MPa H_2) and MCH (●, 3.5 MPa H_2) as a function of inverse temperature at 10 kPa alkane pressure on H*-saturated 0.7 nm Ir clusters.

Taken together, these differences in y and γ reflect the formation of 0.5−1.0 more H_2(g) molecules for ^{3}C−^{x}C than ^{2}C−^{2}C, ^{2}C−^{1}C, or ^{1}C−^{1}C cleavage transition states in 2-MP.

The general nature of these mechanistic inferences and their extension to other noble metals was confirmed by measurements of λ, $\Delta H^{\ddagger}$, and $\Delta S^{\ddagger}$ for ^{1}C−^{1}C bond cleavage in ethane (Table 3)

Table 3. λ, $\Delta H^{\ddagger}$, $\Delta S^{\ddagger}$, and $\Delta G^{\ddagger}$ Values for Cleaving the ^{1}C—^{1}C Bond in Ethane on Hydrogen-Covered Surfaces of Ir, Rh, Ru, and Pt Clusters[a]

catalyst	λ	$\Delta H^{\ddagger}$ (kJ mol^{-1})	$\Delta S^{\ddagger}$ (J mol^{-1} K^{-1})	$\Delta G^{\ddagger}$ (kJ mol^{-1})
0.7 nm Ir	3.0	257	171	156
7 nm Ir	3.3	213	141	129
0.9 nm Rh	3.1	233	161	138
1.0 nm Ru	3.0	197	136	116
0.6 nm Pt	2.2	218	42	193

[a]Values of $\Delta G^{\ddagger}$ are determined from ($\Delta G^{\ddagger} = \Delta H^{\ddagger} - T\Delta S^{\ddagger}$) evaluated at 593 K.

Table 4. λ, $\Delta H^{\ddagger}$, $\Delta S^{\ddagger}$, and $\Delta G^{\ddagger}$ Values for Cleaving the ^{1}C—^{1}C Bond in Isobutane on Hydrogen-Covered Surfaces of Ir, Rh, Ru, and Pt Clusters[a]

catalyst	λ	$\Delta H^{\ddagger}$ (kJ mol^{-1})	$\Delta S^{\ddagger}$ (J mol^{-1} K^{-1})	$\Delta G^{\ddagger}$ (kJ mol^{-1})
0.7 nm Ir	4.0	256	209	132
7 nm Ir	3.8	237	221	105
0.9 nm Rh	4.2	261	252	111
1.0 nm Ru	3.5	194	172	92
0.6 nm Pt	2.5	205	70	163

[a]Values of $\Delta G^{\ddagger}$ are determined from ($\Delta G^{\ddagger} = \Delta H^{\ddagger} - T\Delta S^{\ddagger}$) evaluated at 593 K.

and ^{3}C−^{1}C bond cleavage in isobutane (Table 4) on H*-covered surfaces of Ir (0.7 and 7 nm), Rh (0.9 nm), Ru (1.0 nm), and Pt (0.6 nm) clusters supported on silica. The λ values for ^{3}C−^{1}C cleavage are larger than for ^{1}C−^{1}C bonds on all metals, confirming that the combined number of H* that desorb (γ) and of C−H bonds that cleave (y) in forming ^{3}C−^{x}C cleavage transition states is always larger than for ^{1}C−^{1}C cleavage transition states (and for ^{2}C−^{2}C, and ^{2}C−^{1}C bonds, by analogy with previous data for n-alkane hydrogenolysis on these metals).[11] This leads to $\Delta S^{\ddagger}$ values for ^{3}C−^{1}C cleavage that are, in turn, larger than for ^{1}C−^{1}C cleavage on all metals (Tables 3 and 4). These results indicate that λ and $\Delta S^{\ddagger}$ values are always larger for ^{3}C−^{x}C cleavage than for ^{2}C−^{2}C, ^{2}C−^{1}C, and ^{1}C−^{1}C cleavage, because ^{3}C−^{x}C cleavage transition states are more dehydrogenated and form a larger number of C−M bonds than those involved in the cleavage of C−C bonds containing less substituted C atoms. Thus, the changes in χ values (eq 11) with H_2 pressure (Figure 7) and temperature (Figure 8) seen for 2-MP on small Ir clusters are evident on all other metals as well as on larger Ir clusters.

The larger values of λ and $\Delta H^{\ddagger}$ for ^{3}C−^{x}C bonds relative to those for less substituted C−C bonds in acyclic alkanes (Table 2) are also consistent with rates and selectivities for ring-opening (RO) reactions in arenes and cycloalkanes, which involve cleavage of endocyclic C−C bonds. C−C cleavage rates are smaller for endocyclic ^{3}C−^{x}C bonds, formed by the presence of alkyl substituents in the ring, than for ^{2}C−^{2}C bonds within the ring.[4,6−8,17,18,20,21] Figure 9 shows how C−C bond cleavage rates

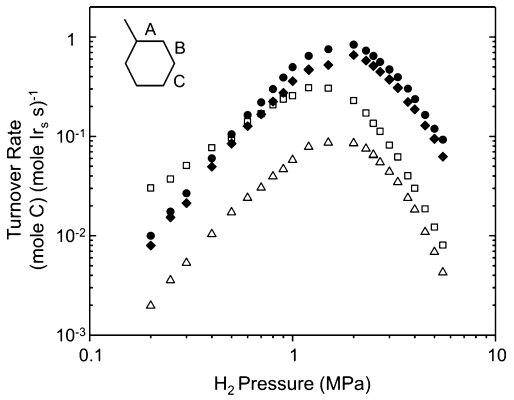

Figure 9. Turnover rates for hydrogenolysis of equilibrated methylcyclohexane-toluene mixtures (MCH) by cleaving ^{2}C−^{2}C (position C, ●), ^{2}C−^{2}C (position B, ◆), ^{3}C−^{2}C (position A, △), and ^{3}C−^{1}C (□) bonds on 0.7 nm Ir clusters at 20 kPa MCH and 593 K.

change with H_2 pressure at each distinguishable C−C bond in equilibrated methylcyclohexane-toluene (MCH) reactant mixtures (20 kPa MCH, 593 K). Transition states that cleave endocyclic ^{2}C−^{2}C bonds (positions B and C, inset Figure 9) have λ values that are nearly identical to those for ^{2}C−^{2}C and ^{2}C−^{1}C bonds in n-alkanes ($\lambda = 3.0 \pm 0.2$, Table 2);[11] in turn, λ values for ^{3}C−^{x}C bonds in MCH are similar to those for ^{3}C−^{x}C bonds in acyclic isoalkanes ($\lambda = 4.0$−4.5, Table 2). These λ values again show that transition states that cleave ^{3}C−^{x}C bonds in cycloalkanes are more dehydrogenated and bind more C atoms to the surface than those involved in ^{2}C−^{2}C bond cleavage. Such findings are consistent with the data and mechanistic inferences reported here for acyclic alkanes (Table 2). The different reactivity and λ values among C−C bonds in MCH give χ values (eq 11), and thus selectivities to branched RO products, that increase with H_2 pressure (Figure 7, as also observed for 2-MP reactants). Figure 8 shows that χ values for MCH (10 kPa MCH, 3.0 MPa H_2, 533−603 K) increase with decreasing temperature, a trend that reflects larger $\Delta H^{\ddagger}$ values for ^{3}C−^{x}C than ^{2}C−^{2}C bonds in MCH (by 30−65 kJ mol^{-1}, Table 2). The changes in χ (i.e., selectivity) with H_2 pressure (Figure 7) and with temperature (Figure 8) resemble those observed with 2-MP

dx.doi.org/10.1021/ja5037429 | J. Am. Chem. Soc. 2014, 136, 9664−9676

reactants (Figures 7, 8), thus confirming the general nature of these mechanistic conclusions and the weak dependence of $\Delta H^{\ddagger}$ and λ values on the structure of chains attached to the C atoms in the cleaved bond.

Figure 10 shows that χ values for MCH increase with H_2 pressure, not only on Ir clusters, but also on Rh, Ru, and Pt

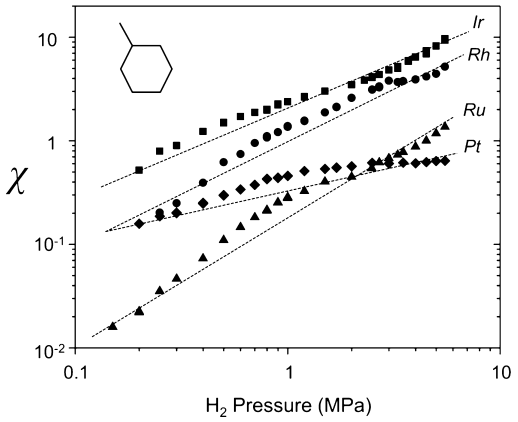

Figure 10. Change in χ for MCH, the ratio of the rate of C−C bond cleavage at unsubstituted (^{2}C−^{2}C) positions to that at substituted positions (^{3}C−^{2}C, ^{3}C−^{1}C), as a function of H_2 pressure on 0.7 nm Ir (■), 0.9 nm Rh (●), 1.0 nm Ru (▲), and 0.6 nm Pt (◆) clusters at 20 kPa MCH, 593 K.

clusters. These similarities confirm that λ values for ^{3}C−^{x}C cleavage transition states are larger than those for cleaving C−C bonds containing less substituted C atoms in cyclic reactants, regardless of the elemental identity of the catalyst.

Overall, the data presented here show that the identity of the alkyl substituent (cyclic or acyclic groups; Figures 7, 8, Table 2), the size of the catalyst cluster (0.7−7 nm; Tables 3, 4), and the elemental identity of the metal catalyst (Ir, Rh, Ru, or Pt; Figure 10, Tables 3, 4) do not influence how H_2 pressure affects the rates of C−C bond rupture at different positions. ^{3}C−^{x}C cleavage always involves transition states that are more deeply dehydrogenated and occupy more surface sites than for less substituted C atoms. These seemingly small differences between transition-state compositions and structures result in values of λ, $\Delta H^{\ddagger}$, and $\Delta S^{\ddagger}$ that are larger for ^{3}C−^{x}C cleavage than for ^{2}C−^{2}C and ^{2}C−^{1}C cleavage in all alkanes, irrespective of chain length, of cyclic or acyclic structure, or of the size and identity of the metal clusters (Ir, Rh, Ru, Pt). These findings are of particular importance because the larger λ, $\Delta H^{\ddagger}$, and $\Delta S^{\ddagger}$ values for ^{3}C−^{x}C bonds compared to ^{2}C−^{2}C and ^{2}C−^{1}C bonds provide practical opportunities to control the extent of branching in hydrogenolysis products through changes in temperature or H_2 pressure. Such effects reflect the structural differences between ^{3}C−^{x}C and ^{2}C−^{2}C bond cleavage transition states, without apparent regard for the secondary structure of the reactant molecules or the elemental identity of the catalytic clusters. It is likely that such consequences extend to reactions that cleave C−X bonds instead of C−C bonds,[57] thus allowing rigorous predictions about the effects of substitution and of reaction conditions on turnover rates and selectivities in desulfurization, denitrogenation, and deoxygenation catalysis (X = S, N, O).

4. CONCLUSIONS

Hydrogenolysis rates for cleaving distinct C−C bonds in isoalkanes, *n*-alkanes, and cycloalkanes measured as functions of alkane and H_2 pressure and temperature show that ^{3}C−^{x}C bond cleavage involves greater λ, $\Delta H^{\ddagger}$, and $\Delta S^{\ddagger}$ values than does ^{2}C−^{2}C and ^{2}C−^{1}C bond cleavage. These differences show that transition states that cleave ^{3}C−^{x}C bonds are more deeply dehydrogenated and less stable (with respect to the gas-phase reactant and H*-covered surfaces) than those for ^{2}C−^{2}C and ^{2}C−^{1}C bonds. These differences arise because ^{3}C atoms cannot occupy high coordination sites (e.g., bridge sites) that bind α,β-bound transition states and that provide the lowest $\Delta G^{\ddagger}$ for ^{2}C−^{2}C, ^{2}C−^{1}C, and ^{1}C−^{1}C bond cleavage. This restriction limits the extent to which electron back-donation to antibonding ^{3}C−^{x}C orbitals weakens the C−C bond: the process responsible for decreasing H_{act} for ^{2}C−^{2}C, ^{2}C−^{1}C, and ^{1}C−^{1}C cleavage with the extent of dehydrogenation. Rather, the dominant ^{3}C−^{x}C cleavage transition states require that three or more C atoms are bound to the surface (e.g., α,β,γ-bound). These transition states for ^{3}C−^{x}C bond cleavage give larger $\Delta H^{\ddagger}$, compared to less substituted C−C bonds, which is consistent with the endothermic nature of the additional dehydrogenation, H* desorption, and C−M bond formation steps that are required to dehydrogenate additional C atoms. Close agreement between measured $S^{\ddagger}$ values and predicted $S^{\ddagger}$ values, based on statistical mechanics treatments of α,β,γ-bound transition states, suggests that such structures are indeed involved in ^{3}C−^{x}C bond cleavage. ^{3}C−^{x}C bond cleavage occurs in these unstable transition states, because their formation produces 1.0−1.5 more $H_2(g)$ molecules, and thus, gives larger entropy gains than for ^{2}C−^{2}C, ^{2}C−^{1}C, or ^{1}C−^{1}C cleavage. The additional $H_2(g)$ increases $\Delta S^{\ddagger}$ values, which at temperatures common for hydrogenolysis (>500 K), significantly decrease $\Delta G^{\ddagger}$. The intrinsic difference between ^{3}C and ^{2}C or ^{1}C atoms in alkanes (i.e., the number of H atoms bonded to each) causes $\Delta H^{\ddagger}$, $\Delta S^{\ddagger}$, and λ values to be consistently greater for ^{3}C−^{x}C bonds than those for ^{2}C−^{2}C and ^{2}C−^{1}C bonds regardless of whether these bonds are contained in branched acyclic or cyclic alkanes or if these reactions occur on Ir, Rh, Ru, or Pt clusters. Such findings show that C−C bonds are weakened on surfaces by forming deeply dehydrogenated structures (i.e., without the need to saturate aromatic structures during ring-opening) and that C atom substitution limits the ability for this to occur (an effect attributed to sterics in many reactions). These realizations provide guidance for hydrotreating processes (where hydrogenation often is quasi-equilibrated) that involve cleaving covalent bonds within organic substrates (e.g., isomerization, hydrodesulfurization (HDS), hydrodeoxygenation (HDO), and hydrodenitrogenation (HDN)) and which aim to control the rates and positions for cleaving C−C bonds and also C−S, C−O, and C−N bonds.

■ ASSOCIATED CONTENT

Supporting Information

Descriptions of the partition functions and assumptions used to calculate entropies of surface species, TEM images and cluster size distributions for the metal cluster catalysts, and plots showing the effects of temperature and H_2 pressure on the hydrogenolysis selectivity of 2,3-dimethylbutane. This material is available free of charge via the Internet at http://pubs.acs.org.

■ AUTHOR INFORMATION

Corresponding Author

iglesia@berkeley.edu

Notes

The authors declare no competing financial interest.

■ ACKNOWLEDGMENTS

The authors acknowledge Dr. Chris Kliewer (ExxonMobil) for obtaining the TEM images and particle size statistics. We also gratefully acknowledge Dr. Elif Gürbüz for measuring hydrogenolysis rates of 2-methylpentane. Partial financial support for this work was generously provided by ExxonMobil Research and Engineering Company.

■ REFERENCES

(1) Weitkamp, J.; Jacobs, P. A.; Martens, J. A. *Appl. Catal.* **1983**, *8*, 123.
(2) Speight, J. G. In *Kirk-Othmer Encyclopedia of Chemical Technology*; Kirk, R. E., Othmer, D. F., Eds.; John Wiley and Sons, Inc.: New York, 2012; p 1.
(3) Iglesia, E.; Reyes, S. C.; Madon, R. J.; Soled, S. L. *Adv. Catal.* **1993**, *39*, 221.
(4) Bond, G. C. *Metal-Catalysed Reactions of Hydrocarbons*; Springer: New York, 2005.
(5) Foger, K.; Anderson, J. R. *J. Catal.* **1979**, *59*, 325.
(6) Weisang, F.; Gault, F. G. *J. Chem. Soc.-Chem. Commun.* **1979**, 519.
(7) McVicker, G. B.; Daage, M.; Touvelle, M. S.; Hudson, C. W.; Klein, D. P.; Baird, W. C.; Cook, B. R.; Chen, J. G.; Hantzer, S.; Vaughan, D. E. W.; Ellis, E. S.; Feeley, O. C. *J. Catal.* **2002**, *210*, 137.
(8) Do, P. T.; Alvarez, W. E.; Resasco, D. E. *J. Catal.* **2006**, *238*, 477.
(9) Anslyn, E. V.; Dougherty, D. A. *Modern Physical Organic Chemistry*; University Science Books: Sausalito, CA, 2006.
(10) McMillen, D. F.; Golden, D. M. *Annu. Rev. Phys. Chem.* **1982**, *33*, 493.
(11) Flaherty, D. W.; Iglesia, E. *J. Am. Chem. Soc.* **2013**, *135*, 18586.
(12) Delbecq, F.; Sautet, P. *Catal. Lett.* **1994**, *28*, 89.
(13) Valcarcel, A.; Clotet, A.; Ricart, J. M.; Delbecq, F.; Sautet, P. *Surf. Sci.* **2004**, *549*, 121.
(14) Yang, M.; Somorjai, G. A. *J. Am. Chem. Soc.* **2004**, *126*, 7698.
(15) Weiss, M. J.; Hagedorn, C. J.; Mikesell, P. J.; Little, R. D.; Weinberg, W. H. *J. Am. Chem. Soc.* **1998**, *120*, 11812.
(16) Zhao, Z.-J.; Moskaleva, L. V.; Rosch, N. *J. Catal.* **2013**, *299*, 146.
(17) Zhao, Z.-J.; Moskaleva, L. V.; Rosch, N. *J. Catal.* **2012**, *285*, 124.
(18) Zhao, Z.-J.; Moskaleva, L. V.; Rosch, N. *ACS Catal.* **2013**, *3*, 196.
(19) Flaherty, D. W.; Hibbitts, D. D.; Gürbüz, E. I.; Iglesia, E. *J. Catal.* **2014**, *311*, 350.
(20) Gault, F. G. *Adv. Catal.* **1981**, *30*, 1.
(21) Anderson, J. R.; D.D. Eley, H. P.; Paul, B. W. *Adv. Catal.* **1973**, *23*, 1.
(22) Watwe, R. M.; Cortright, R. D.; Norskov, J. K.; Dumesic, J. A. *J. Phys. Chem. B* **2000**, *104*, 2299.
(23) Goda, A. M.; Neurock, M.; Barteau, M. A.; Chen, J. G. *Surf. Sci.* **2008**, *602*, 2513.
(24) Bryndza, H. E.; Fong, L. K.; Paciello, R. A.; Tam, W.; Bercaw, J. E. *J. Am. Chem. Soc.* **1987**, *109*, 1444.
(25) Buchanan, J. M.; Stryker, J. M.; Bergman, R. G. *J. Am. Chem. Soc.* **1986**, *108*, 1537.
(26) Karp, E. M.; Silbaugh, T. L.; Campbell, C. T. *J. Am. Chem. Soc.* **2014**, *136*, 4137.
(27) Soled, S. L.; Malek, A.; Miseo, S.; Baumgartner, J.; Kliewer, C.; Afeworki, M.; Stevens, P. A. *Stud. Surf. Sci. Catal.* **2006**, *162*, 103.
(28) Miller, J. T.; Schreier, M.; Kropf, A. J.; Regalbuto, J. R. *J. Catal.* **2004**, *225*, 203.
(29) McVicker, G. B.; Baker, R. T. K.; Garten, R. L.; Kugler, E. L. *J. Catal.* **1980**, *65*, 207.
(30) Cortright, R. D.; Watwe, R. M.; Dumesic, J. A. *J. Mol. Catal. A-Chem.* **2000**, *163*, 91.
(31) Cortright, R. D.; Watwe, R. M.; Spiewak, B. E.; Dumesic, J. A. *Catal. Today* **1999**, *53*, 395.
(32) Cimino, A.; Boudart, M.; Taylor, H. *J. Phys. Chem.* **1954**, *58*, 796.
(33) Kemball, C.; Taylor, H. S. *J. Am. Chem. Soc.* **1948**, *70*, 345.
(34) Morikawa, K.; Benedict, W. S.; Taylor, H. S. *J. Am. Chem. Soc.* **1936**, *58*, 1795.
(35) Sinfelt, J. H.; Yates, D. J. C. *J. Catal.* **1967**, *8*, 82.
(36) Engstrom, J. R.; Goodman, D. W.; Weinberg, W. H. *J. Am. Chem. Soc.* **1988**, *110*, 8305.
(37) Bond, G. C.; Cunningham, R. H. *J. Catal.* **1997**, *166*, 172.
(38) Bond, G. C.; Slaa, J. C. *J. Mol. Catal. A: Chem.* **1996**, *106*, 135.
(39) Chakarov, D. V.; Marinova, T. *Surf. Sci.* **1990**, *227*, 297.
(40) Hill, J. E.; Shen, J.; Watwe, R. M.; Dumesic, J. A. *Langmuir* **2000**, *16*, 2213.
(41) Herron, J. A.; Tonelli, S.; Mavrikakis, M. *Surf. Sci.* **2013**, *614*, 64.
(42) Mavrikakis, M.; Rempel, J.; Greeley, J.; Hansen, L. B.; Norskov, J. K. *J. Chem. Phys.* **2002**, *117*, 6737.
(43) Natal-Santiago, M. A.; Podzolkin, S. G.; Cortright, R. D.; Dumesic, J. A. *Catal. Lett.* **1997**, *45*, 155.
(44) Karp, E. M.; Silbaugh, T. L.; Campbell, C. T. *J. Am. Chem. Soc.* **2013**, *135*, 5208.
(45) Lytken, O.; Lew, W.; Campbell, C. T. *Chem. Soc. Rev.* **2008**, *37*, 2172.
(46) Kua, J.; Faglioni, F.; Goddard, W. A. *J. Am. Chem. Soc.* **2000**, *122*, 2309.
(47) Yeo, Y. Y.; Stuck, A.; Wartnaby, C. E.; King, D. A. *Chem. Phys. Lett.* **1996**, *259*, 28.
(48) Blanksby, S. J.; Ellison, G. B. *Acc. Chem. Res.* **2003**, *36*, 255.
(49) Ford, D. C.; Xu, Y.; Mavrikakis, M. *Surf. Sci.* **2005**, *587*, 159.
(50) Krekelberg, W. P.; Greeley, J.; Mavrikakis, M. *J. Phys. Chem. B* **2004**, *108*, 987.
(51) Hibbitts, D. D.; Flaherty, D. W.; Iglesia, E. to be submitted.
(52) Chorkendorff, I.; Niemantsverdriet, J. W. *Concepts of Modern Catalysis and Kinetics*, 2nd ed.; Wiley-VCH: 2007.
(53) van Santen, R. A.; Neurock, M. *Molecular Heterogeneous Catalysis: A Conceptual and Computational Approach*; Wiley-VCH Verlag GmbH & Co.: Weinheim, 2006.
(54) Yaws, C. L. *Yaws' Handbook of Thermodynamic and Physical Properties of Chemical Compounds*; Knovel: New York, NY, 2003.
(55) http://cccbdb.nist.gov/.
(56) McQuarrie, D. A. *Statistical Mechanics*; University Science Books: Sausalito, CA, 2000.
(57) Sinfelt, J. H. *Catal. Lett.* **1991**, *9*, 159.